1

Spatial and Chromatic Visual Efficiency in Human Neonates

Martin S. Banks
Elizabeth Shannon
University of California at Berkeley

The early stages of vision are primarily serial. Visual stimuli pass sequentially through the eyes' optics, which are responsible for forming the retinal image; the photoreceptors, which sample and transduce the image into neural signals; and two to four retinal neurons, which transform and transmit those signals to the optic nerve and eventually to the central visual pathways. Considerable information is lost in these early stages of the visual process as evidenced by the close correspondence between the filtering properties of the optics and receptors, and some measures of visual sensitivity (e.g., Banks, Geisler, & Bennett, 1987; Coletta, Williams, & Tiana, 1990; Pelli, 1990). In this chapter, we examine how immaturities among these early stages of vision limit the spatial vision and the color vision of human neonates.

It is well established that human neonates see poorly. In the first month of life contrast sensitivity (a measure of the least luminance contrast required to detect a visual target) and visual acuity (a measure of the finest detail that can be detected) are at least an order of magnitude worse than in adulthood (reviewed by Banks & Dannemiller, 1987). Chromatic discrimination (the ability to distinguish targets on the basis of their wavelength composition) is much reduced, too (reviewed by Teller & Bornstein, 1987). One would think that the anatomical and physiological causes of such striking functional deficits would have been identified, but the specific causes are still debated. Some investigators have proposed that optical and retinal immaturities are the primary constraint (Jacobs & Blakemore, 1988; Wilson, 1988), whereas others have emphasized immaturities in the central nervous system (Bronson, 1974; Brown, Dobson, & Maier,

1987; Salapatek, 1975; Shimojo & Held, 1987). Our purpose is to establish as well as possible the limitations imposed by optical and receptor immaturities and to discuss how those limitations should be incorporated into our descriptions and theories of vision in early life. We conclude that much, but not all, of the spatial and chromatic deficits exhibited by neonates can be explained by optical and receptor immaturities. Immaturities among post-receptoral mechanisms are responsible for the unexplained portion of the deficits.

The approach we use relies on ideal observer theory. By definition, the performance of an ideal observer is optimal given the built in physical and physiological constraints (Green & Swets, 1966). Ideal observers have been useful tools in vision research because their performance provides a rigorous measure of the information available at chosen processing stages (Barlow, 1958; Geisler, 1989; Pelli, 1990; Watson, Barlow, & Robson, 1983). For instance, the performance (e.g., contrast sensitivity or visual acuity) of an ideal observer with the optical and photoreceptor properties of an adult eye reveals the information available at the receptors to discriminate various spatial and chromatic stimuli. Similarly, comparing the performance of two ideal observers with different optics and receptors reveals how changes in those properties affect the information available for visual discrimination. In this sense, ideal observer analyses allow an atheoretic assessment of constraints imposed by various stages of visual processing.

Unlike more conventional neural theories that assume specific neural mechanisms at different ages (e.g., Bronson, 1974; Salapatek, 1975; Wilson, 1988), we attempt to reduce assumptions to a minimum. An ideal observer is derived here with the optical and photoreceptor properties of the human neonate (see also Banks & Bennett, 1988). The properties of the young fovea are now understood well enough to minimize the number of necessary assumptions. The performance of this ideal observer is then computed for various spatial and chromatic tasks. Its performance is the best possible for a visual system with the front-end of the newborn system. Moreover, comparisons of the performance of newborn and adult ideal observers reveal the information lost by optical and photoreceptor immaturities across the life span. We will show that much, but not all, of the deficits human neonates exhibit in contrast sensitivity, grating acuity, and chromatic discrimination can be understood from information losses in the optics and photoreceptors.

OPTICAL AND PHOTORECEPTOR DEVELOPMENT

This section briefly reviews the literature on the development of the eye and its optics and on the development of the photoreceptors. More detail is provided in Banks and Bennett (1988).

The eye grows significantly from birth to adolescence, with most of the growth

occurring in the first year. For instance, the distance from the cornea, at the front of the eye, to the retina, at the back (the axial length), is 16 to 17 mm at birth, 20 to 21 mm at 1 year, and 23 to 25 mm in adolescence and adulthood (Larsen, 1971; Hirano, Yamamoto, Takayama, Sugata, & Matsuo, 1979). Shorter eyes have smaller retinal images. So, for example, a 1° target subtends 204 μ (microns) on the newborn's retina and 298 μ on the adult's (Banks & Bennett, 1988). Thus, if newborns had the retina and visual brain of adults, one would expect their visual acuity to be about two thirds that of adults.

Another ocular dimension relevant to visual sensitivity is the diameter of the pupil. The newborn's pupil is smaller than the adult's, but this difference probably has little effect, if any, on visual sensitivity because the eye is shorter, too. More specifically, the eye's numerical *aperture* (the pupil diameter divided by the focal length of the eye) is nearly constant from birth to adulthood (Banks & Bennett, 1988); so, for a given target, the amount of light falling on the retina per degree squared should be nearly constant across age.

Still another ocular factor relevant to visual sensitivity is the relative transparency of the ocular media. Two aspects of ocular media transmittance are known to change with age: the optical density of the crystalline lens pigment and that of the macular pigment. In both cases, transmittance is slightly higher in the young eye, particularly at short wavelengths (Bone, Landrum, Hime, Fernandez, & Martinez, 1987; Werner, 1982). Thus, for a given amount of incident light, the newborn's eye transmits slightly more to the photoreceptors than does the mature eye.

The ability of the eye to form a sharp retinal image is yet another relevant ocular factor. This ability is typically quantified by the *optical transfer function*. There have been no measurements of the human neonate's optical transfer function, but the quality of the retinal image almost certainly surpasses the resolution performance of the young visual system (see Banks & Bennett, 1988, for details). Thus, it is assumed here that the optical transfer function of the young eye is adult-like. This assumption is not critical for our purposes because moderate changes in optical quality would not affect the main conclusions of this chapter.

If optical imperfections do not contribute significantly to the visual deficits observed in young infants, receptoral and postreceptoral processes must. The retina and central visual system all exhibit immaturities at birth (for reviews, see Banks & Salapatek, 1983; Hickey & Peduzzi, 1987), but recent work has also found striking morphological immaturities in the fovea, particularly among the photoreceptors.

The development of the fovea in the first year of life is dramatic, but subtle morphological changes continue until at least 4 years of age (Yuodelis & Hendrickson, 1986). To illustrate some of the more obvious developments, Figs. 1.1 and 1.2 display Yuodelis and Hendrickson's micrographs of retinas at different ages. Figure 1.1 shows low-power micrographs of the fovea at birth, 4 years, and adulthood. The black lines and arrows mark the rod-free portion of the retina,

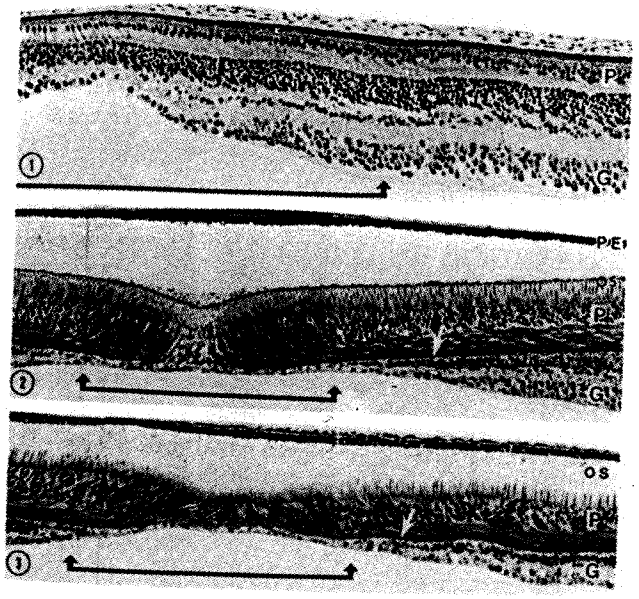

FIG. 1.1. Low-power micrographs of the human fovea at birth (1), 45 months (2), and 72 years (3). The black lines and arrows mark the width of the rod-free foveola. Because at birth the foveola is very wide, only half of it is shown. The most central cone synaptic pedicles are indicated by a white arrow in (2) and (3). P, photoreceptor nuclei; G, ganglion cell layer; OS, outer segment of photoreceptors; PE, pigment epithelium. From Yuodelis and Hendrickson (1986).

the so-called *foveola*. The diameter of the rod-free zone decreases from roughly 5.4° at birth to 2.3° at maturity.

Figure 1.2 displays, at higher magnification, the human foveola at birth and adulthood. An individual cone is outlined for clarity in each panel. The cones' outer segments are labelled OS. The inner segments are just below the outer segments.

In the mature cones, the inner segment captures light, and through waveguide properties, funnels it to the outer segment where the photopigment resides. As the light travels down the outer segment, many opportunities are provided to isomerize a photopigment molecule and thereby create a visual signal.

The micrographs of Fig. 1.2 illustrate the striking differences between neonatal and adult cones. Neonatal inner segments are much broader and shorter, and, unlike their mature counterparts, they are not tapered from the external limiting membrane to the interface with the outer segment. The outer segments are distinctly immature, too, being much shorter than their adult counterparts.

In order to estimate the efficiency of the neonate's lattice of foveal cones, we calculated the ability of the newborn's cones to capture light in the inner

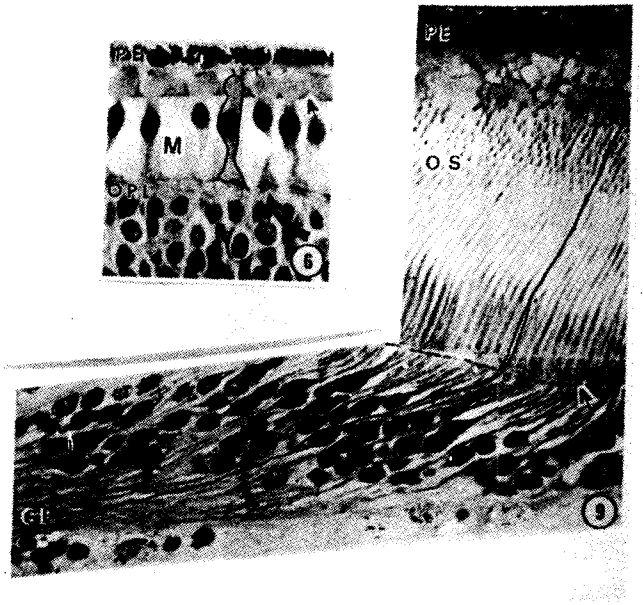

FIG. 1.2. Development of human foveal cones illustrated by light micrographs. A single cone is outlined in both figures; magnification is constant. Ages: (6) = 5 days postpartum; (9) = 72 years. PE, pigment epithelium; OPL, outer plexiform layer; M, Muller glial cell processes; CP, cone pedicles; OS, outer segments. From Yuodelis and Hendrickson (1986).

segment, funnel it to the outer segment, and produce a visual signal (Banks & Bennett, 1988). We began by estimating the effective collecting area of cones at different ages. We found that the newborn inner segment cannot funnel light to the outer segment properly: The inner segment is so short and broad that light rays approaching and reflecting off the inner segment wall at acute angles cannot reach the outer segment.

If the funneling property of the inner segment does not work, the effective aperture or collecting area of newborns' cones must be the outer segment. Taking the smaller size of the newborn eye into account, the angular diameter of the effective collecting area is about 0.35 minutes of arc. The dimensions required to compute this value are given in Table 1.1. The effective aperture of adult foveal cones is, of course, the inner segment because its funneling properties are rather good. Thus, the aperture of adult cones is about 0.48 minutes.

Calculations were also made of the average spacing of cones in the newborn and adult fovea from Yuodelis and Hendrickson's data (see Banks & Bennett, 1988, for details). Table 1.2 shows the cone-to-cone distances in minutes of

TABLE 1.1

Factor	*Source*	*Neonate Central Fovea*	*Neonate Foveal Slope*	*15 Months Central Fovea*	*Adult Central Fovea*
Pupil diameter	Salapatek & Banks (1978)	2.2 mm	2.2 mm	2.7 mm	3.3 mm
Axial length	Larsen (1971) Stenstrom (1946)	16.6 mm	16.6 mm	20.4 mm	24.0 mm
Posterior nodal distance	from axial length ratios	11.7 mm	11.7 mm	14.4 mm	16.7 mm
Receptor aperture	Yuodelis & Hendrickson (1986) Miller & Bernard (1983)	0.35 min arc	0.35 min arc	0.67 min arc	0.48 min arc
Receptor spacing	Yuodelis & Hendrickson (1986)	2.30 min arc	1.66 min arc	1.27 min arc	0.58 min arc

arc. Cone-to-cone separation in the center of the fovea is about 2.3 min, 1.7 min, and 0.58 min in neonates, 15-month-olds, and adults, respectively. It is very important to note that these lattice dimensions impose a limit on the highest spatial frequency that can be resolved without distortion or aliasing (Williams, 1985). This highest resolvable spatial frequency is called the *Nyquist limit*. From cone spacing estimates, Nyquist limits of 15, 27, and 60 c/deg were calculated for newborns, 15-month-olds, and adults, respectively. Adult grating acuity is similar to the Nyquist sampling limit of the foveal cone lattice (Green, 1970; Williams, 1985). One naturally asks, then, whether a similar relationship is observed in newborns. The answer is evident from a comparison of Table 2.2 and Fig. 1.7. Although newborn Nyquist limits are much lower than adult, they are not nearly as low as the highest grating acuity observed early in life. Thus, in human newborns the Nyquist sampling limit of the foveal cone lattice far exceeds the observed visual resolution, implying that coarse sampling by widely spaced receptors is not a major cause of low acuity in newborns.

TABLE 1.2
Nyquist Limits

Assuming regular hexagonal lattice:

$$\textit{Nyquist limit in c/deg} = \frac{60}{\sqrt{3}*D}$$ *where D = center-to-center distance (min arc)*

	D	*Nyquist Limit*
Neonate central fovea	2.30 min arc	15.1 c/deg
Neonate foveal slope	1.66 min arc	20.9 c/deg
15 month central fovea	1.27 min arc	27.2 c/deg
Adult central fovea	0.58 min arc	59.7 c/deg

We used the information listed in Table 1.1 to construct model receptor lattices for newborns and adults; these are shown in Fig. 1.3. The white bars at the bottom of each panel represent 0.5 minutes of arc and serve as references. The light gray areas represent the effective collecting areas: the cone apertures. Nearly all of the light falling within these apertures reaches the photopigment and is, therefore, useful for vision. The effective collecting areas cover 65% and 2% of the retinal patches for the adult and newborn foveas, respectively. Consequently, the vast majority of incident photons are not collected within newborn cone apertures and are, therefore, not useful for vision.

The next factor to consider is how efficiently the outer segment—where the photopigment resides—absorbs photons and produces the isomerization that

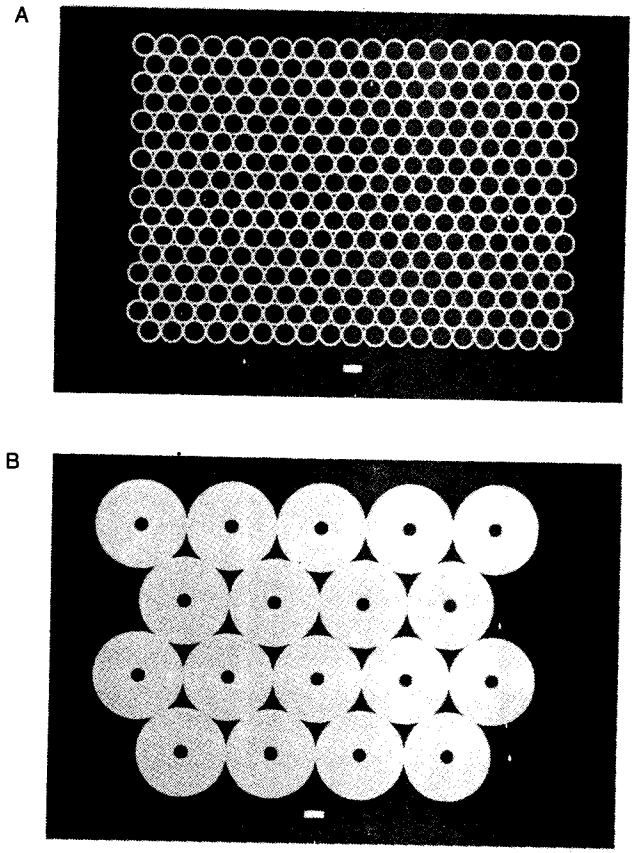

FIG. 1.3. Schematics of the receptor lattices used in (a) adult and (b) neonatal ideal observers. The white bars represent 0.5 min arc. Light gray areas represent the inner segments; dark gray areas represent effective collecting areas. The effective collecting areas cover 65% of the adult central fovea but only 2% of the newborn central fovea.

triggers the visual process. As can be seen in Fig. 1.2, the lengths of newborn and adult outer segments differ substantially. In the central fovea, for instance, the ratio of adult to newborn outer segment length is about 16:1. Intuitively, longer outer segments should provide more opportunities for a photon to produce an isomerization. We calculated the proportion of photons incident on the outer segment that produce an isomerization (see Banks & Bennett, 1988, for details). The 16:1 difference calculated between adult and newborn outer segment lengths produces about a 10:1 difference in the number of isomerizations for a given number of incident photons. These calculations imply that once photons are delivered to outer segments, newborn cones are much less efficient than mature cones in producing isomerizations.

One can see from these calculations that the cone lattice of the newborn fovea is quite inefficient in delivering photons to the photopigment-laden outer segments. Moreover, because the path length of the outer segment is short, its efficiency is low, too. Taking into account the age-related changes in the factors listed in Table 1.1, we estimate that the adult foveal cone lattice absorbs 350 times more quanta than the newborn foveal lattice. Stated another way, if identical patches of light are presented to newborn and adult eyes, roughly 350 photons are effectively absorbed in adult foveal cones for every photon absorbed in newborn cones.

Ideal observers were built for the adult fovea and newborn fovea. The properties built into these observers are listed in Table 1.1. All of the ideal observers had three receptor types—SWS (short-wavelength-sensitive or blue), MWS (medium-wavelength-sensitive or green), and LWS (long-wavelength-sensitive or red) cones—with adult spectral sensitivities (Estevez, 1979; Walraven, 1974). SDE software developed by Geisler (1984) was used to compute the performance of these observers for various spatial and chromatic tasks. As mentioned earlier, ideal observers employ an optimal decision rule to discriminate stimuli on the basis of different effective photon catches among photoreceptors. Thus, they allow one to assess, without assumptions about subsequent neural mechanisms, the limitations optical and receptoral properties place on the detection and discrimination of spatial and chromatic stimuli. Likewise, the performance of the neonatal ideal observer relative to the adult is a measure of the extra information lost by immature optics and photoreceptors.

CONTRAST SENSITIVITY

The *contrast sensitivity function* (CSF) represents the visual system's sensitivity to sinusoidal gratings of various spatial frequencies. The CSF is a reasonably general index of visual sensitivity because any two-dimensional pattern can be represented by its spatial frequency content (Banks & Salapatek, 1981; Cornsweet, 1970). Thus, an understanding of how optical and receptoral immaturities limit contrast sensitivity should offer insight into how they limit spatial vision in general.

Before discussing infant contrast sensitivity, consideration is given to how optics and photoreceptor efficiency affect contrast sensitivity in adults. Banks et al. (1987) and Crowell and Banks (1991) used the ideal observer whose properties are detailed in Table 1.1 to calculate the best contrast sensitivity the human fovea could possibly have given the quantal fluctuations in the stimulus (photon noise), the optics of the eye, and the size, spacing, and efficiency of the foveal cones. They also included considerations of a postreceptoral factor: the functional summation area for gratings of different spatial frequencies (Howell & Hess, 1978). (Summation experiments suggest that the intermediate- to high-frequency detecting mechanisms summate information over a constant number of grating bars or cycles.)

Figure 1.4 displays the CSF of the ideal observer for sinewave gratings of a constant number of cycles. Different functions illustrate the contributions of various pre-neural factors. The function labeled *quantal fluctuations* represents the performance of an ideal machine with no optical defocus and arbitrarily small and tightly packed photoreceptors. This function has a slope of -1, which is to say that contrast sensitivity is inversely proportional to patch width. The inverse proportionality is a manifestation of the square-root law behavior of ideal machines (Banks et al., 1987; Barlow, 1958; Rose, 1942). The function labeled *aperture and quantal fluctuations* represents performance when the photoreceptors are given the dimensions of the adult foveal cones; comparing it to the one above it reveals the contribution of the finite aperture of foveal cones (which has the effect of attenuating high spatial frequencies slightly). The solid lines represent performance with all pre-neural factors included; the difference between this function and the one above it represents the contribution of optical defocus (Campbell & Gubisch, 1967). The other solid lines represent the contrast sensitivities for luminances of 340, 34, and 3.4 cd/m^2. As expected for ideal machines, these functions follow the square-root law: Reducing luminance by a log unit produces a half log unit reduction in contrast sensitivity.

Figure 1.5 shows the performance of real adult observers when they are presented the same targets as the ideal observer. The data points are contrast sensitivities for gratings of 5 to 40 c/deg for two adult observers. As is normally observed, contrast sensitivity is greater for high than for low luminances. As expected, the contrast sensitivity values for the real adult observers are substantially lower than those of the ideal observer.

The solid lines are the three ideal functions of Fig. 1.4 shifted vertically as a unit to fit the real observer's data. The ideal functions fit the experimental data reasonably well, which shows that the shapes of the ideal and real CSFs are similar. The similarity of shapes demonstrates that the high-frequency roll-off of the human adult's foveal CSF for gratings with a fixed number of cycles can be explained by the operation of optical and receptoral factors alone. This observation implies, in turn, that neural efficiency—the efficiency with which information at the outputs of the receptors is transmitted through the rest of

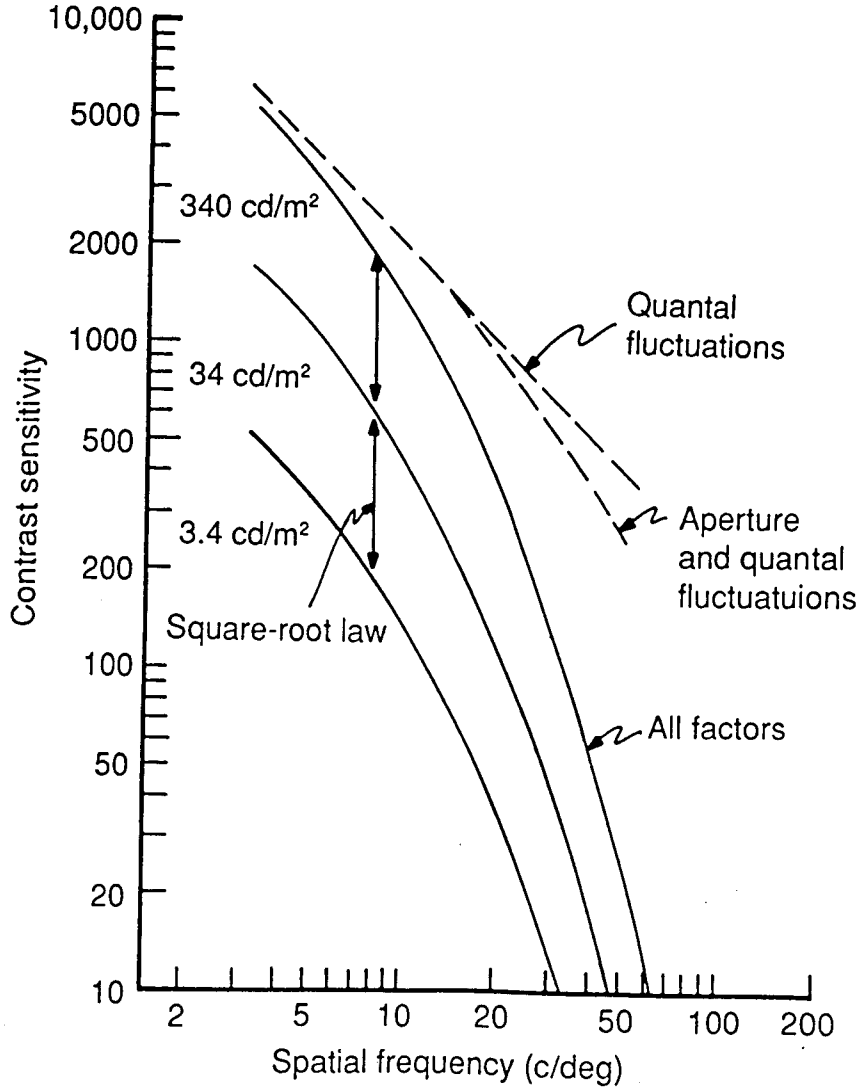

FIG. 1.4. CSF of an ideal observer incorporating different properties of the human adult fovea. Contrast sensitivity is plotted against the spatial frequency of fixed-cycle sine-wave grating targets. The highest dashed curve shows the contrast sensitivity of an ideal machine limited by quantal noise, ocular media transmittance, and photoreceptor quantum efficiency. The slope of -1 is dependent on the use of sine-wave gratings of a constant number of cycles. Space-average luminance is 340 cd/m^2. The lower dashed curve shows the contrast sensitivity with the receptor aperture effect included. Finally, the highest solid curve shows the sensitivity with the optical transfer function added. The other solid curves represent the contrast sensitivities for 34 and 3.4 cd/m^2. From Banks, Geisler, and Bennett (1987).

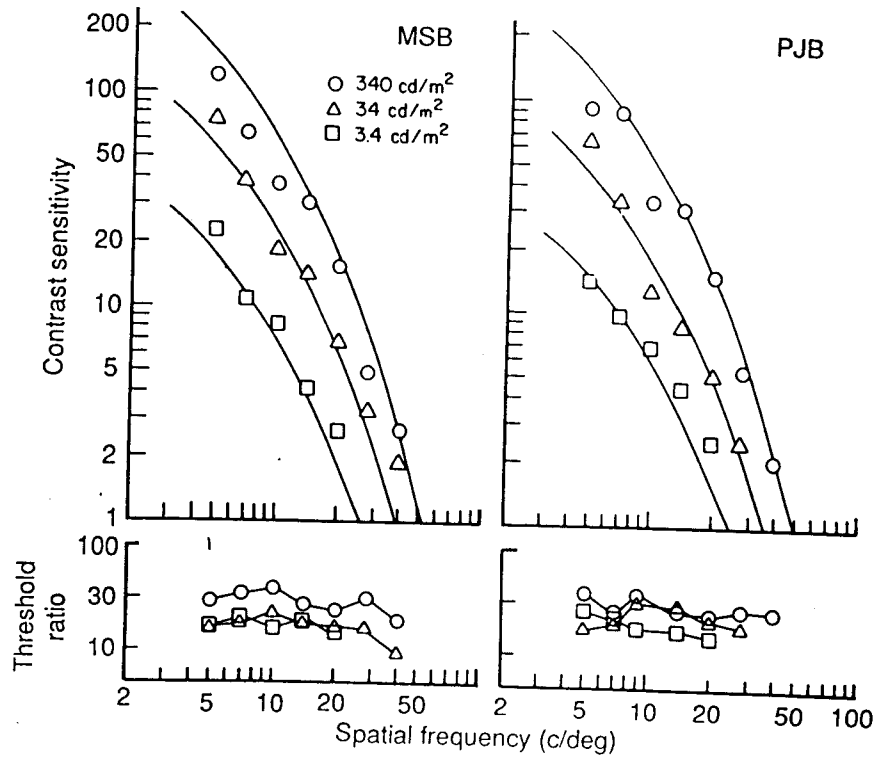

FIG. 1.5. Contrast sensitivity functions of two adult observers. The top graphs plot contrast sensitivity as a function of spatial frequency for three luminance levels tested. The solid lines are the contrast sensitivity of the ideal observer (from Fig. 1.4), shifted downward by 1.33 log units for MSB and 1.43 log units for PJB. The bottom graphs plot threshold ratios as a function of spatial frequency. The ratios are the human observers' contrast threshold divided by the ideal observer's thresholds. From Banks, Geisler, and Bennett (1987).

the visual system—is constant from 5 to 40 c/deg for adult foveal vision. Moreover, the luminance dependance of intermediate- and high-frequency sensitivity is similar for real and ideal adult observers, which means that adults exhibit square-root behavior just like ideal observers. These two observations—that the spatial-frequency dependence and luminance dependence of human adult contrast sensitivity is similar to those exhibited by an ideal observer placed at the receptors—are important in our analysis of contrast sensitivity development: They legitimize comparisons of ideal and real observer performance at different ages.

Figure 1.6 displays neonatal and adult CSFs. Contrast sensitivity is obviously quite low in newborns. Peak sensitivity, whether measured by forced-choice preferential looking (FPL; Atkinson, Braddick, & Moar, 1977; Banks & Sala-

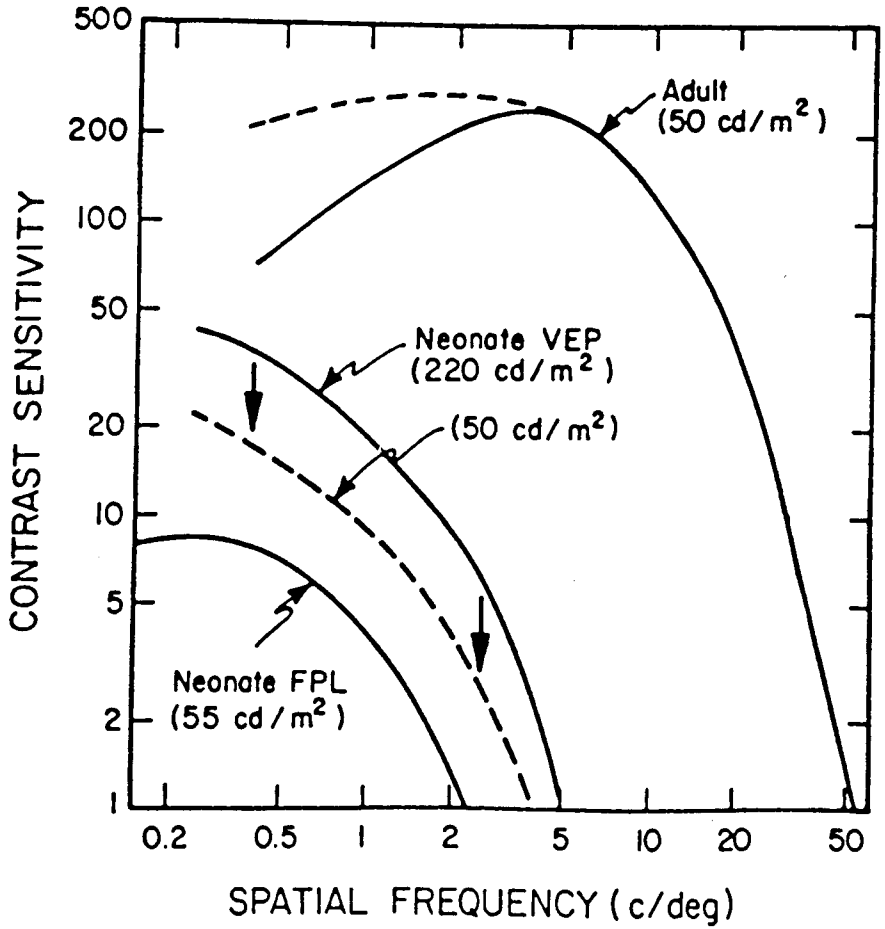

FIG. 1.6. Empirically determined adult and infant CSFs and the predicted loss of sensitivity caused by optical and receptoral factors. The function labeled Neonate FPL is from Banks and Salapatek (1978). The function labeled Neonate VEP is from A. M. Norcia (personal communication, 1988). The dotted line indicates the expected location of the VEP function at 50 cd/m^2, assuming the square-root law holds. The function labeled Adult is from Campbell and Robson (1968); the dashed extension to it indicates the presumed sensitivity for counterphase flickering gratings like those used in VEP studies.

patek, 1978) or by the visual evoked potential (VEP; Norcia, Tyler, & Allen, 1986; Pirchio, Spinelli, Fiorentini, & Maffei, 1978), is substantially lower than that of adults. One can also see that visual acuity in neonates is very limited, being 12 to 25 times worse than that of normal adults (Dobson & Teller, 1978; Norcia & Tyler, 1985).

To examine the extent to which the development of contrast sensitivity can be explained by optical and receptoral maturation, CSFs of the ideal neonatal

and adult observers were computed for gratings of a fixed number of cycles. The space-average luminance was 50 cd/m^2. The ideal CSFs are shown in Fig. 1.7. As in Fig. 1.4, these functions reflect performance limitations imposed by quantal fluctuations in the stimulus, ocular media transmittance, optical transfer, and the aperture spacing, efficiency, and spacing of photoreceptors. Notice that the ideal sensitivity is higher at the margin of the newborn's foveola than in the central 250 μ because of the greater efficiency of foveal slope cones (that is, cones roughly 2.7° from the center of the fovea; see Table 1.1 and Banks & Bennett, 1988, for details).

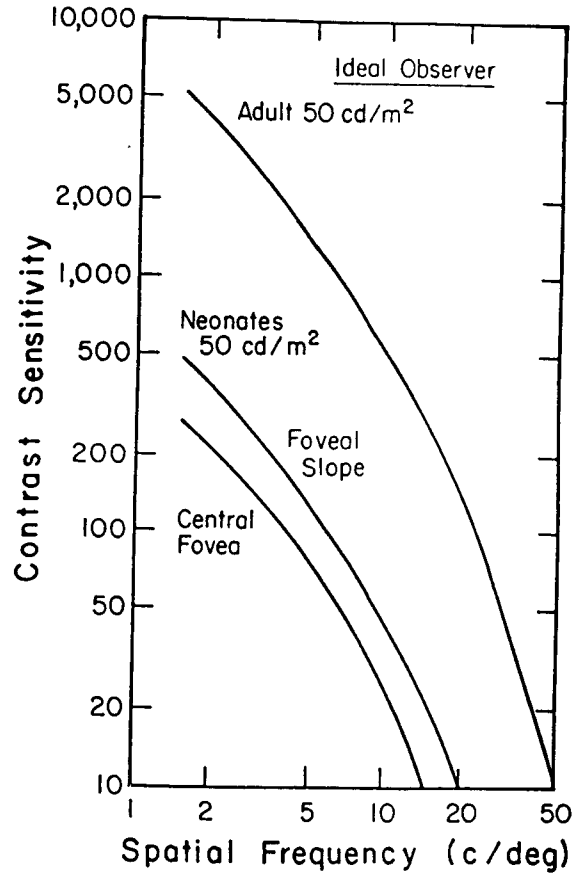

FIG. 1.7. CSFs for ideal observers incorporating the pre-neural factors of the adult and neonatal central foveas and the neonatal foveal slope. As in Fig. 1.4, the stimuli were grating patches of a constant number of cycles, in order to incorporate changes in summation area with spatial frequency (Banks, Geisler, & Bennett, 1987; Howell & Hess, 1978). Space-average luminance is 50 cd/m^2. The differences between adult and neonatal sensitivities are due primarily to the reduced quantum capture of the neonate's cone lattice. From Banks and Bennett (1988).

Most noteworthy are the differences between the contrast sensitivities of the adult and neonatal ideal observers. They are substantial. For example, the ratio between adult sensitivity and neonatal central foveal sensitivity at 5 c/deg is about 21:1 (1.32 log units). The major cause of decreased sensitivity in the newborn is the reduced photon capture of its cone lattice.

Of course, neither adults nor newborns are ideal observers, so one naturally asks whether these predicted differences in sensitivity can explain the differences observed between real adult and real newborn performance. If the visual systems of newborns and adults were identical except for the observed differences in eye size, and in cone aperture, efficiency, and spacing, one would expect the neonatal CSF to be simply a vertically shifted version of the adult. To examine this possibility, empirically determined adult and newborn CSFs were compared. Figure 1.8 displays an adult CSF at 50 cd/m^2 along with neonatal CSFs obtained at similar luminances with FPL and VEP. The vertical arrows indicate the amount of shifting one would expect if the visual systems of adults and newborns were identical except for the optical and receptoral factors listed in Table 1.1. The vertical shifts correspond to information lost by small eye size and inefficient photon capture and photoisomerization. As already mentioned, the fact that ideal and real adult contrast sensitivities are affected in similar ways by changes in spatial frequency and luminance makes plausible the implicit assumption behind vertical shifting. In keeping with this, the adult function was not shifted at frequencies below 3 c/deg because Banks et al. (1987) and Crowell and Banks (1991) were unable to show that differences between real and ideal contrast sensitivity below 3 c/deg can be explained by the factors considered.

The shifting accounts for a substantial fraction of the observed newborn–adult disparity, but not all of it. Evidently, additional factors contribute to the newborn contrast sensitivity deficit. The disparity between the real newborn CSF and the shifted adult function will be called the *postreceptoral gap*. It is illustrated in Fig. 1.9. Our analysis suggests that the postreceptoral loss is roughly 7-fold (0.85 log units) at 3 c/deg and 22-fold (1.34 log units) at 5 c/deg. What factors, not considered in our analysis, determine the magnitude and shape of the postreceptoral gap? There are, of course, numerous candidates including intrinsic neural noise (such as random addition of action potentials at central sites), inefficient neural sampling (such as lack of appropriate cortical receptive fields for detecting sinewave gratings), poor motivation to respond, and so forth.

A caveat is warranted before concluding this section. Despite the fact that the fovea subtends a large area at birth, newborns may use extrafoveal loci in contrast sensitivity experiments. There are no quantitative data on the morphological development of extrafoveal cones, so it is possible that the extrafoveal cones are actually more efficient than foveal cones at birth (Abramov et al., 1982). If this were the case, the disparity between predicted and observed contrast sensitivity (the postreceptoral gap) would be greater than indicated in Figs. 1.8 and 1.9. There is some evidence, however, that suggests, but by no means

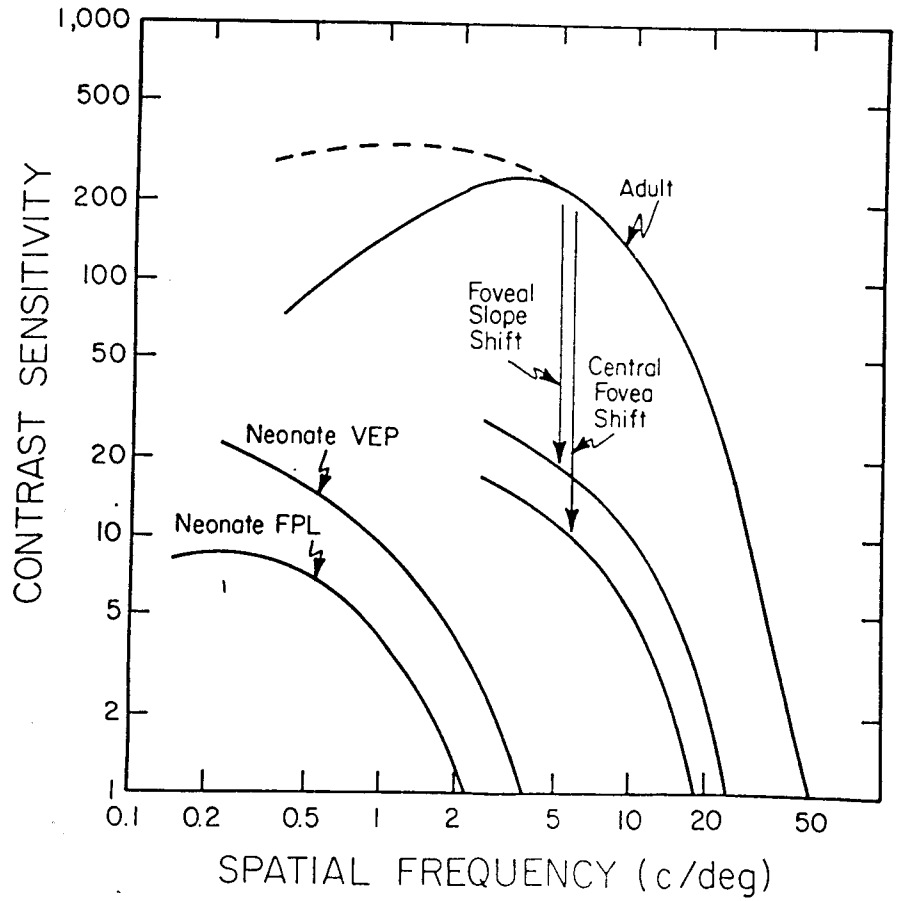

FIG. 1.8. Empirically determined adult and infant CSFs and the predicted loss of sensitivity caused by optical and receptoral factors. The curve labeled Neonate FPL is from Banks and Salapatek (1978) and was collected at 55 cd/m^2. The curve labeled Neonate VEP is derived from data from A. M. Norcia (personal communication, 1988). The VEP data were collected at a space-average luminance of 220 cd/m^2, so we shifted the functions downward by 0.32 log unit to indicate its expected location at 50 cd/m^2 (under the assumption that the square-root law holds). The curve labeled Adult represents data from Campbell and Robson (1968) that were collected at 50 cd/m^2. Each vertical arrow represents the ratio of the ideal neonate sensitivity to the ideal adult sensitivity at each spatial frequency. The reductions in contrast sensitivity indicated by the arrows represent the effects of smaller image magnification, coarser spatial sampling by the cone lattice, and less efficient photoreception in the neonate. The curves at the bottom of the arrows are the CSFs that one would expect if adult and neonatal visual systems were identical except for pre-neural factors. From Banks and Bennett (1988).

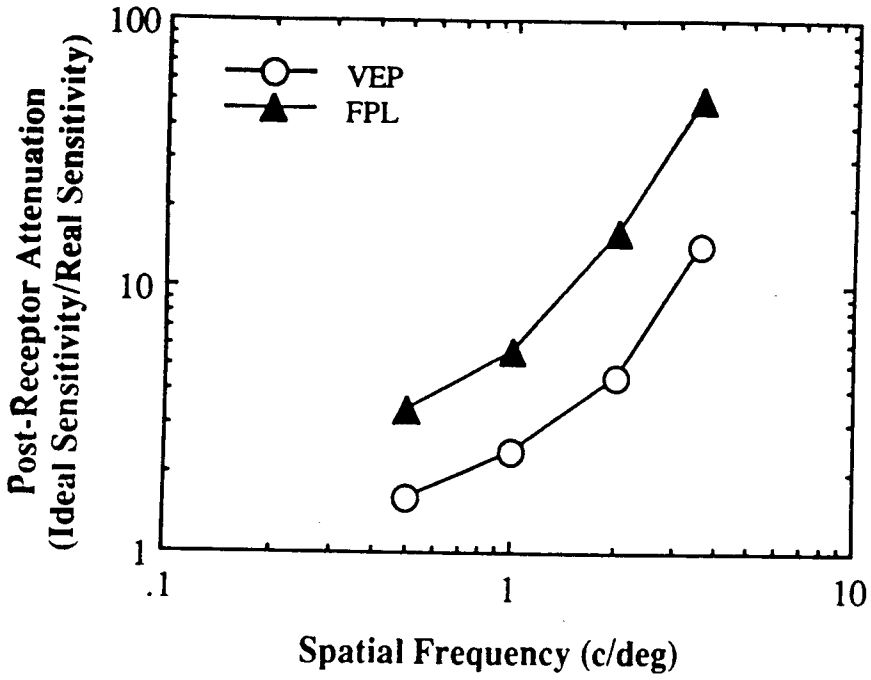

FIG. 1.9. The postreceptoral gap. The ratio of predicted/observed infant contrast sensitivity is plotted as a function of spatial frequency. The predicted sensitivities are the shifted curves in Fig. 1.8 and represent the contrast sensitivities one would expect if the only loss of information infants suffer relative to adults is due to immature optics and photoreceptors.

proves, that newborns fixate visual targets foveally. Hainline and Harris (1988), Slater and Findlay (1975), and Salapatek and Kessen (1966) all showed that neonates use a consistent retinal locus when fixating a high-contrast target. They could not, however, prove that this locus is the fovea because of uncertainties about the location of the visual axis with respect to the optic axis. Other evidence relevant to the issue of peripheral and foveal viewing concerns the relative sensitivity of foveal and peripheral vision in neonates; some of this evidence is from macaques, and some is from humans. Retinal and central nervous development in macaques and humans is similar, except that macaques are somewhat more advanced at birth and mature more rapidly (Boothe, Williams, Kiorpes, & Teller, 1980; Hendrickson & Kupfer, 1976; Kiely et al., 1987). Blakemore and Vital-Durand (1980) measured the visual resolution of lateral geniculate cells supplied by different retinal regions. In newborn macaques, the acuity of foveal cells was similar but higher than the acuity of peripheral cells. Thus, in macaque infants, the highest resolution is likely to be observed with central vision. The same appears to be true for human infants. Lewis, Maurer, and

Kay (1978) found that newborns could detect a narrower light bar against a dark background when it was presented in central vision than when it was presented in the periphery. More recently, Allen, Norcia, and Tyler (1989) showed that VEP acuity is higher in central than in peripheral vision in infants as young as 2 months. These observations suggest that the newborn contrast sensitivity and acuity estimates are manifestations of central rather than peripheral processing, but more direct experimental evidence is needed to show that central fixation is the same as foveal fixation in such young infants.

In conclusion, within the assumptions of the analysis just presented, much but not all of the contrast sensitivity and acuity deficits observed early in life can be accounted for by small eye size and by photoreceptor immaturities in and around the fovea. The major constraint is the poor photon catching of the newborn's foveal cone lattice. The unexplained portion of the sensitivity deficit—the postreceptoral gap—must reflect immaturities among postreceptoral retinal circuits and central visual pathways.

CHROMATIC VISION

We next investigated whether changes in visual efficiency, as indexed by the comparison of human neonate to ideal observer performance, offer much insight into the development of chromatic vision.

Infants less than 8 weeks of age do not consistently demonstrate the ability to discriminate stimuli that differ in hue only. Older infants, however, make such discriminations quite reliably (Clavadetscher, Brown, Ankrum, & Teller, 1988; Hamer, Alexander, & Teller, 1982; Packer, Hartmann, & Teller, 1984; Peeples & Teller, 1975; Teller, Peeples, & Sekel, 1978; Varner, Cook, Schneck, McDonald, & Teller, 1985). Here we consider three sorts of hue discriminations—Rayleigh, tritan, and neutral-point—because they are particularly interesting theoretically.

The *neutral-point* test is based on the observation that color-normal, trichromatic adults are able to distinguish all spectral (monochromatic) lights from white; that is, they do not exhibit a neutral point. In contrast, color-deficient observers, such as dichromats, exhibit distinct neutral points. Peeples and Teller (1975) and Teller et al. (1978) used a neutral-point test to examine 8-week-olds' color vision. They examined both white-on-white luminance discrimination and discrimination of a variety of chromatic targets from white. The stimulus conditions are listed in Table 1.3 and the colors of the test targets and background are represented in Fig. 1.10, which is a chromaticity diagram. Eight-week-olds discriminated many colors from white: red, orange, some greens, blue, and some purples (see also Table 1.3). They did not, however, discriminate yellow, yellow-green, one green, and some purples from white. Thus, 8-week-old infants seemed to exhibit a neutral zone running from short wavelengths to yellow and

TABLE 1.3

Experiment	*Age*	*Task*	*Stimuli*	*Results*	*Ratio*	*Predicted Weber Fraction*	*Accurate Prediction*
Hamer et al. (1982)	4 weeks	Chromatic	Red on yellow	Fail	3.49	1.92	+
			Green on yellow	Fail	3.14	1.73	+
	8 weeks	Chromatic	Red	Marginal	3.49	1.27	+
			Green	Marginal	3.14	1.13	+
	12 weeks	Chromatic	Red	Pass	3.49	0.63	+
			Green	Pass	3.14	0.57	+
Packer et al. (1984)	4 weeks	Intensity	Yellow(8°×8°)	Threshold = ± .27 lu			
		Chromatic	Red(8°×8°)	Fail	3.49	1.61	+
		Intensity	Yellow(4°×4°)	Threshold = ± .35 lu			
		Chromatic	Red(4°×4°)	Fail	3.49	1.92	+
		Intensity	Yellow(2°×2°)	Threshold = ± .55 lu			
		Chromatic	Red(2°×2°)	Fail	3.49	2.51	+
	12 weeks	Intensity	Yellow(8°×8°)	Threshold = ± .11 lu			
		Chromatic	Red(8°×8°)	Pass	3.49	0.54	+
		Intensity	Yellow(4°×4°)	Threshold = ± .18 lu			
		Chromatic	Red(4°×4°)	Pass	3.49	0.63	+
		Intensity	Yellow(2°×2°)	Threshold = ± .31 lu			
		Chromatic	Red(2°×2°)	Marginal	3.49	1.08	+
		Intensity	Yellow(1°×1°)	Threshold = ± .40 lu			
		Chromatic	Red(1°×1°)	Fail	3.49	1.40	+
Peeples & Teller (1975)	8 weeks	Intensity	White(14°×1°)	Threshold = ± .12 lu			
		Chromatic	Red on white	Pass	2.58	0.62	+
Teller et al. (1978)	8 weeks	Intensity	White(14°×1°)	Threshold = ± .12 lu			
		Chromatic	Red on white	Pass	2.58	0.62	+
			Orange	Pass	4.13	1.00	+
			Yellow 1	Marginal	12.26	2.95	+
			Greenish-yellow	Fail	7.10	1.71	+
			Yellowish-green	Fail	4.17	1.01	+
			Green 1	Marginal	3.29	0.79	–
			Green 2	Pass	3.23	0.78	+
			Greenish-blue	Pass	2.90	0.70	+
			Blue	Pass	2.52	0.61	+
			Bluish-purple	Pass	7.35	1.78	–
			Purple 1	Fail	10.32	2.49	+
			Purple 2	Marginal	9.94	2.39	+
			Reddish-purple	Pass	3.42	0.83	+
Varner et al. (1985)	4 weeks	Intensity	Green (4°×4°)	Threshold = ± .16 lu			
		Chromatic	Violet on green	Fail	0.04	0.01	–
	8 weeks	Intensity	Green	Threshold = ± .10 lu			
		Chromatic	Violet on green	Pass	0.07	0.01	+
Clavadetscher et al. (1988)	3 weeks	Intensity	Green(8°×8°)	Threshold = ± .40 lu			
		Chromatic	Violet 1 on green	Fail	0.04	0.02	–
		Chromatic	Violet 2 on green	Fail	0.07	0.04	–
		Chromatic	Blue on green	Fail	0.84	0.50	–
		Chromatic	Red on green	Marginal	1.98	1.19	+
		Chromatic	Blue on red	Marginal	2.85	<1.71	+
	7 weeks	Intensity	Green(8°×8°)	Threshold = ± .20 lu			
		Chromatic	Violet 1 on green	Pass	0.04	0.01	+
		Chromatic	Violet 2 on green	Marginal	0.07	0.02	–
		Chromatic	Blue on green	Pass	0.84	0.31	+
		Chromatic	Red on green	Pass	1.98	0.73	+
		Chromatic	Blue on red	Pass	2.85	<1.05	+

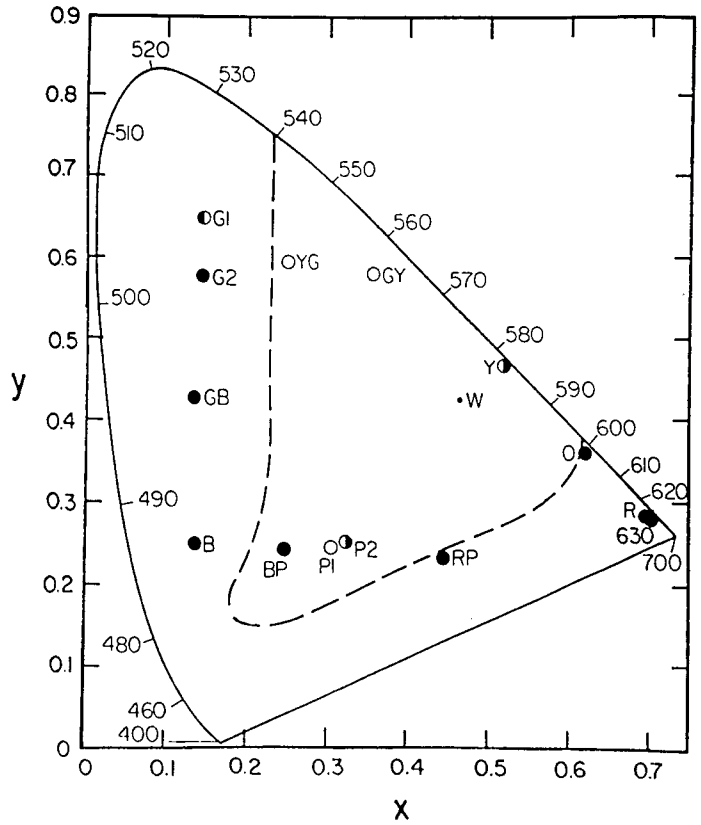

FIG. 1.10. Chromaticities of the stimuli used in the neutral-point experiment of Peeples and Teller (1975) and Teller et al. (1978). Subjects in both experiments were 8-week-old infants. Filled symbols represent stimuli that all infants reliably discriminated from white (W); open symbols represent hues that all infants failed to discriminate from white; half-filled symbols represent hues that some, but not all, infants discriminated from white. The dashed curve represents the boundary between hues that should and hues that should not be discriminated from white according to the visual efficiency hypothesis. Hues falling outside the triangular area bounded by the dashed curve should be discriminable from white, and those falling within the area should not. From Banks and Bennett (1988).

green. Although they included other possibilities, Teller et al. (1978) hypothesized from these results that 8-week-olds may have deficient SWS cones because the neutral zone was somewhat similar to that exhibited (in color parlance) in tritanopia or tritanomalous trichromacy.

A *tritan* test is designed to examine the function of SWS cones. By presenting two lights that activate MWS and LWS cones equally, the test isolates the SWS cones. Varner et al. (1985) asked whether 4- to 8-week infants could distinguish two such lights. Specifically, they presented violet targets in a green

surround. Table 1.3 lists the conditions. Eight-week-olds distinguished the two lights at all luminances, so they must have at least minimally functional SWS cones. Four-week-olds, on the other hand, did not discriminate the two lights reliably, suggesting an SWS cone defect or a postreceptoral defect involving the circuits serving the SWS cones.

Rayleigh discrimination tests involve the discrimination of brightness-matched, long-wavelength lights, such as red and green. They are diagnostically important because adults with the most common color defects—*deuteranopia* (lacking MWS cones) and *protanopia* (lacking LWS cones)—are unable to make such discriminations. Hamer et al. (1982) and Packer et al. (1984) examined the ability of 4-, 8-, and 12-week-olds to make Rayleigh discriminations. The stimulus conditions are described in Table 1.3. Either a green or a red target was presented at one of a variety of luminances on a yellow surround. The results were clear-cut: Most 8-week-olds and essentially all 12-week-olds made these discriminations reliably. This is clear evidence that most infants have at least minimally functional LWS and MWS cones by 8 weeks of age. In contrast, the majority of 4-week-olds did not exhibit the ability to make either discrimination. Packer et al. also found a significant effect of target size. Twelve-week-olds were able to make Rayleigh discriminations with 4° and 8° targets, but not 1° and 2° targets. These results imply that the color vision of 4-week-olds differs from that of color-normal adults, perhaps due to an absence of MWS and/or LWS cones or to an inability of postreceptoral circuits to compare MWS and LWS cone signals. The target-size effect in older infants suggests that the stimulus must be salient for them to demonstrate their chromatic ability.

More recently, Clavadetscher et al. (1988) re-examined the conditions tested by Hamer et al. (1982), Packer et al. (1984), and Varner et al. (1985) along with some new conditions. Specifically, they used the same paradigm employed in the previous work to examine 3- and 7-week-olds' ability to distinguish pairs of monochromatic lights. The conditions are listed in Table 1.3. In the first experiment, test lights of 645 nanometers (nm) (red), 486 nm (blue), 446 nm (blue), or 417 nm (violet) were presented against a 547 nm (green) background. In the second experiment, a light of 486 nm was presented against a broadband red background. Thus, there were five hue pairings tested in all. Three-week-olds did not discriminate any of these pairings reliably, but they gave evidence of a modest ability to discriminate the 645/547 nm and 486 nm/red pairings. Seven-week-olds discriminated all of the pairings reliably. Thus, the observations of Clavadetscher et al. (1988) confirm the earlier reports in that their neonates did not exhibit the ability to make Rayleigh (e.g., 645/547 nm) nor tritan (417/547 nm) discriminations reliably. They extend these observations, however, by showing that neonates also fail to discriminate other hue pairings reliably.

We should add, because it is important for the theoretical analyses described later in this section, that Teller and her colleagues also measured luminance discrimination thresholds in each of the aforementioned experiments by measur-

ing the smallest luminance increments and decrements required to elicit a reliable response.

Teller and her colleagues have drawn the following conclusions from this constellation of data: First, most infants are probably trichromatic by 12, if not 8, weeks of age; that is, they have three functional cone types and the postreceptoral machinery required to preserve and compare their signals. Second, at 4 weeks of age, the majority of infants fail to make both Rayleigh and tritan discriminations and therefore have some form of color deficiency. Teller and her co-workers raised the possibility that younger infants' discrimination failures may be due to the absence or relative immaturity of different cone types or because of relative immaturities among postreceptoral chromatic channels.

In sum, there are no rigorous demonstrations that the majority of infants 4 weeks of age or younger make hue discriminations. The absence of such evidence is consistent with the hypothesis that human neonates are generally color deficient. Two sources of such deficiency are possible: First, neonates may track only one or two cone types or one or two of their cone types may be insensitive relative to the other cone types. Second, neonates may lack postreceptoral chromatic channels or have less sensitive chromatic channels compared to their luminance channels.

There is, however, another possibility. Perhaps neonates have a full complement of functional, although inefficient, cone types and the requisite neural machinery to preserve and compare their signals, but their overall visual efficiency is simply too poor to allow them to demonstrate their chromatic capabilities. Similarly, older infants may exhibit reliable chromatic discrimination because of increased visual efficiency. For the purposes of this hypothesis, we define *visual efficiency* as the discrimination performance of a visual system limited by optical and photoreceptor properties (see Tables 1.1 and 1.2) plus a general postreceptoral loss. This definition will be made clearer further on.

The visual efficiency hypothesis is evaluated by using the ideal observer whose properties are given in Table 1.1 and a measure of visual efficiency. To introduce the approach, adults' luminance and chromatic discrimination is first discussed. Mullen (1985) measured adults' luminance contrast sensitivity with monochromatic gratings (yellow and black stripes) of various spatial frequencies and chromatic sensitivity with isoluminant (equally bright) red/green and blue/yellow gratings. She found that luminance contrast sensitivity exceeded chromatic sensitivity by a factor of 4 to 5 at most spatial frequencies. An important question is whether reduced chromatic contrast sensitivity at intermediate to high spatial frequencies reflects reduced sensitivity among post-receptoral chromatic channels as opposed to luminance channels or whether it simply reflects reduced *cone contrast* (the variation in photon catch from one cone to the next), due to the overlapping spectral sensitivities of different cone types.

To address this question, Geisler (1989) computed the performance of an adult ideal observer for the conditions of Mullen's experiment. The observer

had a full complement of LWS, MWS, and SWS cones with adult properties. Naturally, the contrast sensitivity of the ideal observer was much higher than the sensitivity of Mullen's observers, but the effects of spatial frequency and chromatic versus luminance contrast were quite similar: The shapes of real and ideal luminance CSFs and real and ideal chromatic CSFs were nearly identical across a wide range of spatial frequencies. Moreover, ideal luminance sensitivity was consistently 3.5 times greater than ideal chromatic sensitivity for the colors chosen. Geisler concluded, therefore, that the contrast sensitivities of real and ideal adult observers are affected similarly by the spatial frequency and chromatic content of the stimulus. Because the ideal observer had no postreceptoral channels devoted to luminance or chromatic contrast, this observation shows that different efficiencies among such channels need not be hypothesized to explain the difference between luminance and chromatic contrast sensitivity.

Why is the ideal observer's sensitivity poorer for an isoluminant chromatic grating than for a luminance grating? The main cause is the extensive spectral overlap of cone photopigments.[1] Because of the overlap, the modulation of LWS and MWS cone outputs is significantly reduced for isoluminant chromatic gratings as compared to luminance gratings composed of the same components. The diminished cone response is bound to reduce ideal sensitivity because ideal observers utilize all the information in the matrix of cone signals. The fact that real observers show similar sensitivity losses over a wide range of spatial frequencies suggests that the extensive spectral overlap of cone types is a major constraint on human adult chromatic contrast sensitivity, too.

Geisler's conclusion can be expressed in a simple fashion: The ratio of adult chromatic sensitivity to adult luminance sensitivity is equal to the corresponding ratio of ideal sensitivities. This same reasoning can be applied to infants' color vision: The visual efficiency hypothesis, described earlier in a qualitative fashion, can now be stated quantitatively: Infant chromatic sensitivity divided by infant luminance sensitivity is also equal to the corresponding ratio of ideal sensitivities (and, therefore, to the ratio of adult sensitivities).

We adapted the ideal observer analysis to ask whether the visual efficiency hypothesis is consistent with empirical observations of early chromatic vision and its development. First, the sensitivity of the infant ideal observer was computed for the experimental conditions of Teller and her colleagues. The observer

[1]To explain this, it is useful to consider an isoluminant red/green grating divided into its two components: a red/black grating and a green/black grating. Consider, in particular, the outputs of LWS cones to each grating component. When the red component is presented, LWS cones respond in rough proportion to the luminance variation from the peak to the trough of the grating. They also respond in this way to the green component, although their responses at peaks and troughs are somewhat reduced. When the red and green grating components are added in phase—producing a yellow/black grating—the LWS cone modulations due to each component add, producing a large overall modulation. However, when the components are combined in opposite phase—producing an isoluminant red/green grating—the LWS cone modulations of each component cancel to some degree and the overall modulation is smaller. The same reasoning obviously applies to the MWS cones.

was identical to the one whose properties are given in Table 1.1. In keeping with the hypothesis that infants have a normal complement of cone types, we built in SWS, MWS, and LWS cones in adult proportions and with adult spectral sensitivities (see Banks & Bennett, 1988, for details), but each cone type was made less efficient than its adult counterpart in keeping with the earlier observations on contrast sensitivity.

After constructing the infant ideal observer, the spectral characteristics of each stimulus were encoded and the corresponding activations of SWS, MWS, and LWS cones calculated. This allowed us to compute the infant ideal observer's thresholds for the luminance and chromatic discrimination tasks of the five experiments listed in Table 1.3. Ideal luminance discrimination threshold was expressed as the just-detectable luminance decrement divided by the background luminance. To compute ideal chromatic discrimination performance, we constructed a stimulus composed of the uniform background, a decrement in the background, and an increment of the appropriate color. For example, the computer version of the Rayleigh stimulus of Packer et al. (1984) consisted of a uniform yellow background and a square region of the same luminance with a yellow decrement and a red increment. The increment was added in various proportions around the presumed equiluminance point in order to find the luminance ratio for which threshold was highest. While maintaining isoluminance, the magnitudes of the decrement and increment were manipulated in order to establish the infant ideal observer's chromatic discrimination threshold. This threshold was expressed as a Weber fraction: the magnitude of the background decrement (in this case, the yellow decrement) divided by the background luminance. Finally, the ratio of the ideal Weber fraction for chromatic discrimination divided by the ideal Weber fraction for luminance discrimination was computed. The ratios for each age group and experimental condition are given in Table 1.3. Higher ratios mean higher chromatic thresholds. The ratios vary widely from color to color. The smallest was 2.52, for blue-on-white discrimination, and the largest was 12.3, for yellow-on-white discrimination.

The ideal observer's luminance discrimination thresholds were much lower than those of Teller's infants. Furthermore, the neonate ideal observer was able to make all of the chromatic discriminations when the contrast of the target (background decrement/background luminance) was 1.0 as it was in Teller's experiments. Thus, as with contrast sensitivity and grating acuity, the infant ideal observer exhibited notably better performance than real neonates. Earlier, this performance disparity was attributed to postreceptoral losses.

The visual efficiency hypothesis outlined earlier incorporates such postreceptoral losses. It states that young infants' inability to make chromatic discriminations is a manifestation of low visual efficiency rather than some deficit among chromatic mechanisms per se. In other words, luminance and chromatic sensitivity should, according to this hypothesis, follow similar growth curves. Predictions of the visual efficiency hypothesis are obtained simply by multiplying the

observed luminance discrimination thresholds (the Weber fractions measured by Teller and her colleagues) by the ratio of ideal chromatic to ideal luminance threshold. In equations, the predictions are:

$$CT_n/LT_n = CT_i/LT_i \quad (1)$$

$$CT_n = CT_i*(LT_n/LT_i) \quad (2)$$

where CT_n and LT_n are the chromatic and luminance thresholds (Weber fractions) for neonates and CT_i and LT_i are the same for the ideal observer. For examples of these predictions, refer to Table 1.3. In the Packer et al. (1984) experiment, for instance, the observed luminance discrimination threshold of 4-week-olds was 0.27 log units, a Weber fraction of 0.46. The ratio of ideal chromatic/luminance threshold was 3.49. So the chromatic discrimination Weber fraction (or threshold contrast) predicted by the visual efficiency hypothesis is simply 0.46×3.49, or 1.61. But for Teller's stimuli (background decrements replaced by increments of a different hue), contrasts greater than 1.0 are not physically realizable, so the hypothesis predicts a discrimination failure. The predicted thresholds vary with age, luminance, and target size because the luminance discrimination thresholds reported by Teller and her colleagues varied with those factors. Consequently, the hypothesis makes the unsurprising prediction that chromatic discrimination improves with increasing luminance, target size, and age. The predictions varied with the colors of the background and test target, too, because the ratios of ideal chromatic to ideal luminance threshold depended on the spectral composition of the stimuli. Thus, some discriminations, such as yellow from white, are expected to be more difficult than others, like blue from white.

The predicted Weber fractions for the neutral-point tests of Peeples and Teller (1975) and Teller et al. (1978) are given in the next to last column of Table 1.3. The visual efficiency hypothesis predicts discrimination failures for predicted Weber fractions greater than 1.0 and successes for smaller fractions. Figure 1.10 depicts the neutral-point predictions and data in the format of the chromaticity diagram. The data points represent the stimuli and the dashed line the predictions. The filled data points represent colors that were always discriminated by 8-week-olds, and unfilled points represent those colors that the infants always failed to discriminate. Half-filled points are those colors that were occasionally discriminated. Colors within the line should, according to the hypothesis, be indiscriminable from white, and colors outside the line should be reliably discriminated. The zone of theoretically indiscriminable stimuli is broad and, as expected, it does not resemble confusion zones for any standard dichromatic observer because the infant ideal observer has three cone types. The predictions match the observations tolerably well. We conclude that 8-week-olds' performance in the neutral-point experiments of Peeples and Teller (1975) and Teller et al. (1978) is largely consistent with the predictions of the visual efficiency hypothesis.

The predictions for the Rayleigh discrimination experiments (Hamer et al., 1982; Packer et al., 1984) are also given in Table 1.3 and illustrated in Figs. 1.11 and 1.12. Consider the experiment of Packer et al. first. Again, empirical measurements of luminance discrimination thresholds were multiplied by the ratio of ideal chromatic to ideal luminance threshold to estimate the Weber fractions, which, according to the hypothesis, would be needed for reliable discrimination (see Banks & Bennett, 1988, for details). These fractions are plotted in Fig. 1.11 and listed in the next to last column of Table 1.3. The dotted line represents chromatic contrasts of 1.0, the value presented in the Packer et al. experiment. Filled symbols represent those conditions in which discriminations were made reliably and unfilled symbols conditions in which discriminations were consistently not made. Half-filled symbols represent conditions in which the discrimination was made occasionally. All of the fractions for 4-week-olds are greater than 1.0, so the hypothesis correctly predicts discrimination failures for all target sizes at that age. The 12-week data and predictions are more complicated.

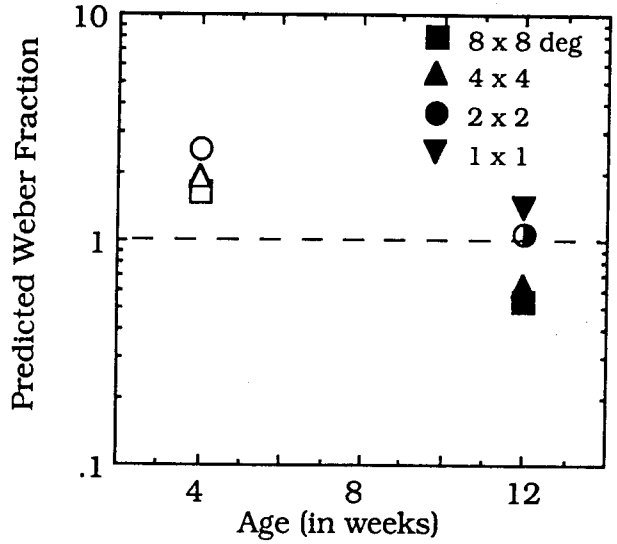

FIG. 1.11. Data and predictions for the Packer et al. (1984) experiment. Predicted Weber fractions are plotted as a function of age in weeks. Open symbols represent conditions in which infants did not reliably discriminate the test pair. Filled symbols represent conditions in which infants exhibited reliable discrimination, and half-filled symbols represent conditions in which some infants exhibited reliable discrimination and some did not. Different symbol shapes represent different target sizes. The dashed line represents the contrasts of the stimuli presented in this experiment. The vertical placement of the symbols corresponds to the Weber fractions predicted by the visual efficiency hypothesis. Thus, symbols above the dashed line represent conditions in which discrimination failures are predicted, and symbols below the line represent conditions in which reliable discrimination is predicted.

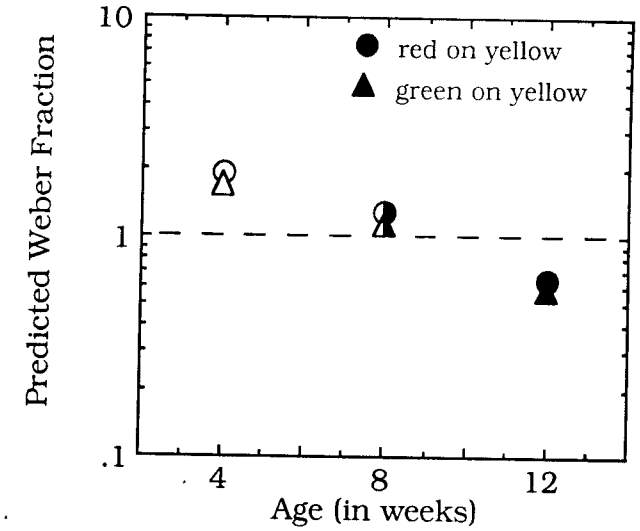

FIG. 1.12. Data and predictions for the Hamer et al. (1982) experiment. Conventions are the same as in Fig. 1.11, except that different symbols represent green-on-yellow and red-on-yellow discriminations.

The fractions are less than 1.0 for 4° and 8° targets, so the hypothesis predicts reliable discrimination for those targets. The fraction is slightly greater than unity for the 2° target, so a near miss is predicted. Finally, the fraction is well above unity for the smallest target, so a discrimination failure is predicted. The efficiency hypothesis, therefore, correctly predicts the results in all three conditions at 4 weeks and all four at 12 weeks.

Now consider the other Rayleigh discrimination experiment by Hamer et al. (1982). Figure 1.12 displays the empirical observations and the predictions of the efficiency hypothesis. The predicted Weber fractions are well above unity for 4-week-olds, so the efficiency hypothesis correctly predicts clear discrimination failures for red and green targets at that age. The fractions are slightly greater than 1.0 for 8-week infants, so near misses are predicted. Finally, the fractions are well below unity for the oldest infants, so consistent discrimination is correctly predicted for both colors at that age.

The predictions of the visual efficiency hypothesis are consonant with the pattern of Rayleigh discriminations observed by Hamer et al. (1982) and Packer et al. (1984). Recall that the neonatal ideal observer used in deriving predictions has three equally functional cone types and uses optimal strategies to compare their outputs. Stated another way, the efficiency hypothesis assumes no deficit among chromatic mechanisms relative to luminance mechanisms. Thus, poor Rayleigh discrimination performance early in life does not necessarily imply deficiencies among chromatic mechanisms per se. The pattern of discrimi-

nation failures observed among the youngest children and for small targets among the older children can be explained by the operation of optical and receptoral factors, and changes overall visual efficiency alone.

We have shown that two hypotheses can account for neonates' inability to make Rayleigh discriminations. The first, which we call the *chromatic deficiency hypothesis*, claims that neonates lack MWS and/or LWS cones, or one is much less efficient than the other, or have a deficit among their red/green postreceptoral chromatic mechanisms. The second, the *visual efficiency hypothesis*, claims that neonates have functional MWS and LWS cones and the requisite red/green mechanisms, but that these are too insensitive to support Rayleigh discriminations.

The chromatic deficiency hypothesis predicts that Rayleigh discrimination performance should improve with age more than luminance discrimination performance: specifically, that the ratio CT/LT (see equation 2) decreases with age. The cause of the decrease could be receptoral or postreceptoral in origin. A receptoral cause would be the absence of one or two cone types or lower efficiency in one or two cone types compared to the remaining ones. A postreceptoral cause would be the absence of the red/green and/or blue/yellow chromatic mechanism or lower sensitivity among one or two chromatic mechanisms relative to the luminance mechanism.

The visual efficiency hypothesis predicts that chromatic and luminance sensitivities should both increase with age, but the ratio of sensitivities should remain constant. The visual efficiency hypothesis states that the ratio of efficiencies among cone types is similar across age (all are less efficient than their adult counterparts) and that the ratio of sensitivities of postreceptoral chromatic and luminance mechanisms is similar across age (all less efficient than adult mechanisms). In order to distinguish these two hypotheses, more sensitive measurements of chromatic discrimination are needed.

To this end, Allen, Banks, Norcia, and Shannon (1990) used VEPs, which provide higher contrast sensitivities than FPL, and optimal spatiotemporal stimuli to examine luminance and Rayleigh discriminations at different ages. The stimuli consisted of two spatial sinusoids of equal contrast: one produced by modulating a saturated green stimulus (thus creating a green/black grating) and the other by modulating a saturated red stimulus (creating a red/black grating). The two sinusoids were added in spatial counterphase (the bright red bars of one sinusoid being positioned in between the bright green bars of the other). They then varied the ratio of R/(R+G), where R and G are the mean luminances of the red and green sinusoids. R/(R+G) ratios of 0, 0.5, and 1.0 yielded green/black, red/green, and red/black sinusoids, respectively.[2]

[2]The stimuli were created by modulating the green and red guns of a Conrac 7300 display. Allen et al. placed an amber filter in front of the CRT screen in order to minimize the contribution of SWS cones and to insure that the stimuli were in the Rayleigh region, above 550 nm. The CIE chromaticity coordinates of the filtered green and red phosphors were (0.42, 0.57) and (0.65, 0.34), respectively. Space-average luminance was 8 cd/m^2.

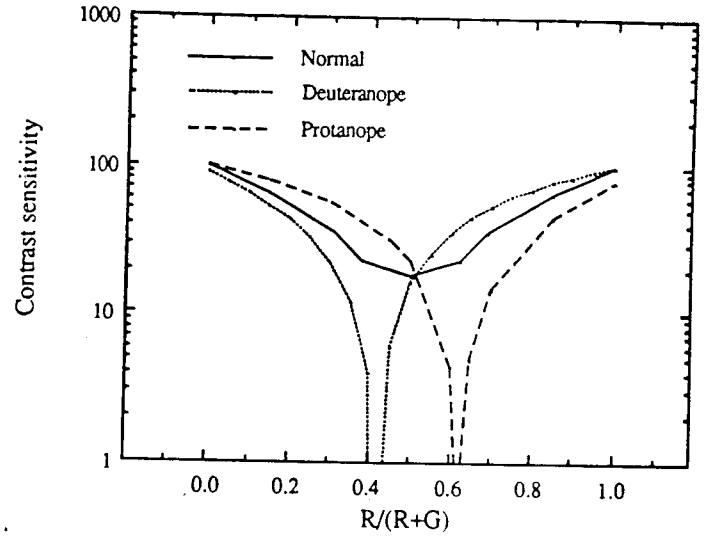

FIG. 1.13. Predictions of contrast sensitivity as a function of the amount of red in a red/green sinusoidal grating. The solid line is the predicted sensitivity of a normal trichromatic observer. The prediction was calculated from an ideal observer with SWS, MWS, and LWS cones in the ratio of 1:16:32. The dotted line is the prediction for a deuteranope and the dashed line is the prediction for a protanope. The prediction is that the grating will be undetectable by the deuteranope at an R/(R+G) value of .42 and undetectable by a protanope at a value of .62. From Allen et al. (1990).

Figure 1.13 displays the contrast sensitivity values one predicts for color-normal and color-deficient observers. The solid line represents the predicted contrast sensitivity for a normal trichromatic observer. The prediction was calculated from the adult ideal observer with a full complement of SWS, MWS, and LWS cones. The dotted line represents the predicted sensitivities for a deuteranope, a person who lacks MWS cones, and the dashed line represents the predicted sensitivities for a protanope, who lacks LWS cones. Allen et al. (1990) found that the psychophysical and VEP data of color-normal adults are consistent with the predictions for a color-normal observer.

Figure 1.14 displays the sensitivity values obtained in three color-defective adults. Panel A shows data from two protanopes. The open circles are psychophysical thresholds and the squares are thresholds obtained with VEPs. These protanopes showed a large decrement in performance at the predicted R/(R+G) ratio of 0.62. Panel B shows the data for a protanomalous observer who also shows a performance dip in the expected region, but because she has some functional LWS cones, the dip is not as large as the protanopes'.

The visual efficiency hypothesis predicts that the shapes of the solid-line functions in Figs. 1.13 and 1.14 will be the same in neonates and normal adults, but that the neonatal functions will be displaced downward on the log sensitivity

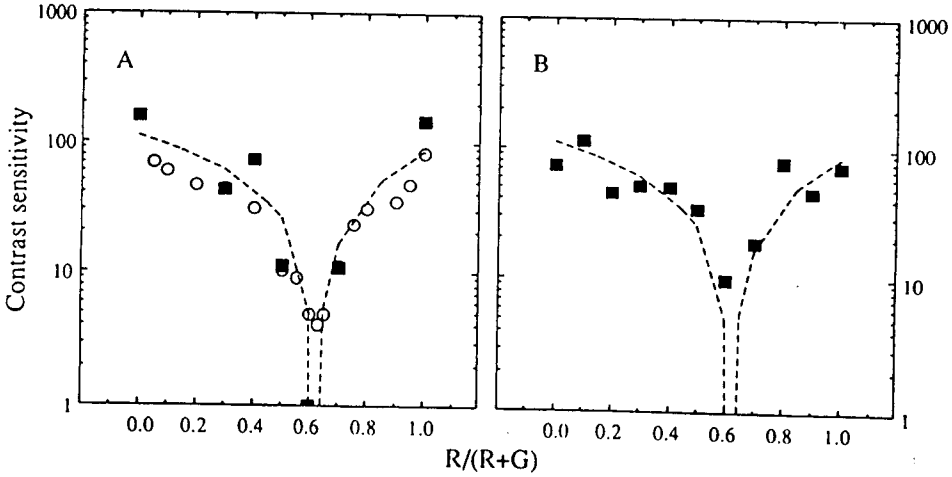

FIG. 1.14. Contrast sensitivity in color-deficient adults. Panel A shows thresholds from two protanopic adults. The open circles are psychophysical thresholds and the closed squares are thresholds estimated from sweep VEP recordings. The dashed line is the predicted sensitivity for a protanope. The data point on the x-axis at 0.6 represents the absence of a VEP signal at that value. Panel B shows VEP thresholds from a protanomolous adult. Like the protanope, the protanomolous adult has a dip in sensitivity close to the value predicted for an observer lacking LWS cones. However, at this value VEPs are measurable in the protanomolous adult. From Allen et al. (1990).

axis. The chromatic deficiency hypothesis, on the other hand, predicts that the shapes of the functions will differ for neonates and adults: The dip should be larger in neonates, more like the color-deficient adults in Fig. 1.14.

Allen et al. (1990) tested neonates from 2 to 7 weeks of age using the VEP. The data from 4 of these children are displayed in Fig. 1.15 along with the prediction for a color-normal individual. In each case, the data are consistent with the predictions for a color-normal observer and clearly inconsistent with those for protanopes and deuteranopes. The data from 13 infants who completed at least six threshold measurements are shown in Fig. 1.16. Again, these data are inconsistent with predictions for a protanope or deuteranope. The data are also inconsistent with the idea that the red/green postreceptoral chromatic mechanism in neonates is less mature than the postreceptoral luminance mechanism; if it were less mature, the dip in these functions would be larger in neonates than in adults.

Allen et al. (1990) concluded that infants as young as 2 weeks of age demonstrate a clear cortical response to an isoluminant red/green grating. This observation is consistent with the visual efficiency hypothesis that young infants' inability to demonstrate chromatic discriminations behaviorally (e.g., Hamer et al., 1982) is due to generally poor visual sensitivity rather than to a loss of LWS

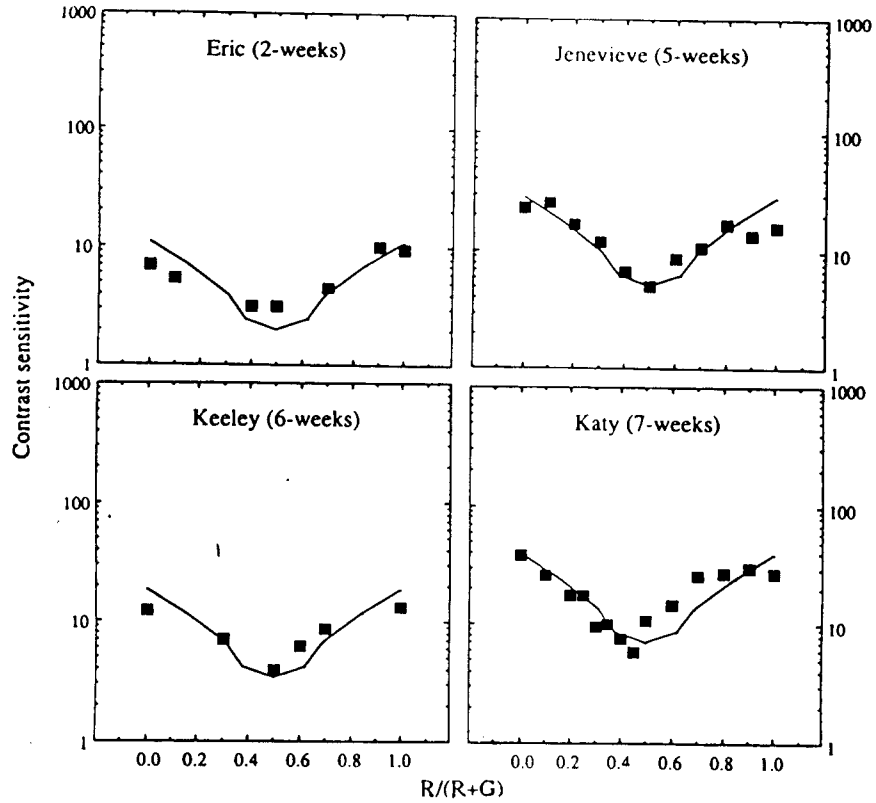

FIG. 1.15. Contrast sensitivity in four infants from 2 to 7 weeks of age. The spatial frequency of the grating was 0.8 c/deg. The solid lines are the predicted sensitivity of a normal trichromatic observer. Thresholds were obtained from sweep VEP recordings. From Allen et al. (1990).

or MWS cones or a specific immaturity of the postreceptoral red/green mechanism. Thus, human neonates appear to have functional MWS and LWS cones and the postreceptoral neural machinery to preserve and compare their signals.

We now turn to a discussion of tritan discriminations, which isolate the functioning of SWS cones, and, to some extent, the postreceptoral blue/yellow chromatic mechanism. Varner et al. (1985) reported that few 4-week-olds and most 8-week-olds demonstrate the ability to make a tritan discrimination. We again examined the performance of the infant ideal observer in the conditions of this experiment. In contrast to the Rayleigh and neutral-point discriminations discussed earlier, chromatic performance near isoluminance actually exceeded luminance performance. That is, the threshold Weber fraction of the ideal observer was lower for discrimination of violet from green near isoluminance than for discrimination of a green decrement alone. This behavior occurred because the ideal observer used a different strategy in this chromatic task than it had in the

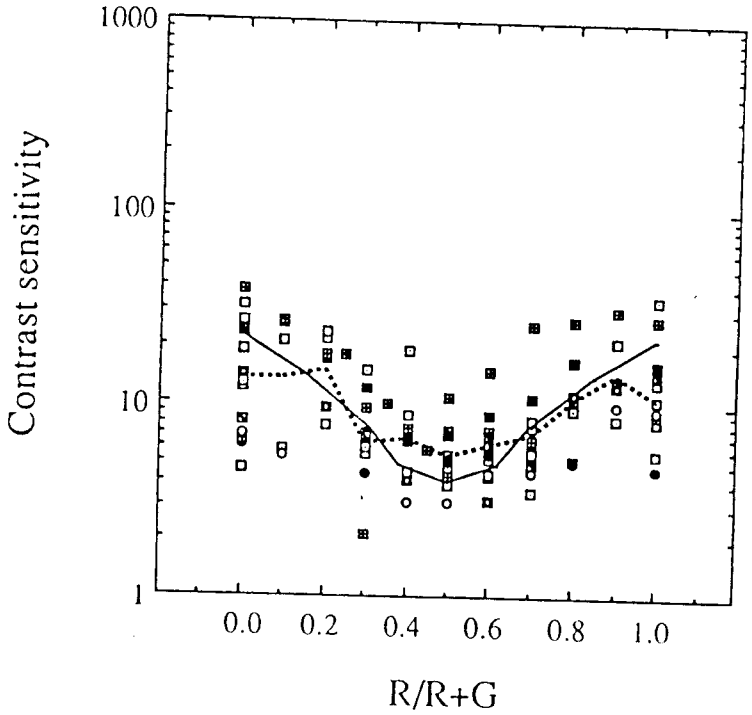

FIG. 1.16. Contrast sensitivity for 13 infants from 2 to 7 weeks of age. The solid line is the predicted sensitivity of a normal trichromatic observer. The dashed line connects the means at each value of R/(R+G). From Allen et al. (1990).

others. Color-normal adults actually exhibit similar behavior (for details, see Banks & Bennett, 1988), so the visual efficiency hypothesis cannot predict the pattern of results observed in 4-week-olds. The prediction failure for 4-week-olds is indicated by the minus sign in the rightmost column of Table 1.3. This observation implies that infants may well have a tritan color defect: dysfunctional or relatively insensitive SWS cones or relatively insensitive blue/yellow chromatic mechanisms. Of course, this prediction failure does not affect our interpretation of the Rayleigh discrimination experiments because they do not involve SWS cones.

To examine further the possibility that infants 4 weeks of age or less have a tritan defect, we looked at the results of Clavadetscher et al. (1988). They reported that 3-week-olds fail to discriminate a variety of lights (417, 448, 486, and 645 nm) from green, and blue (486 nm) from red. Seven-week-olds in their study made all of these discriminations reliably. The predictions of the visual efficiency hypothesis were computed as before and they are listed in Table 1.3 and displayed in Figure 1.17. The figure plots the predicted Weber fraction

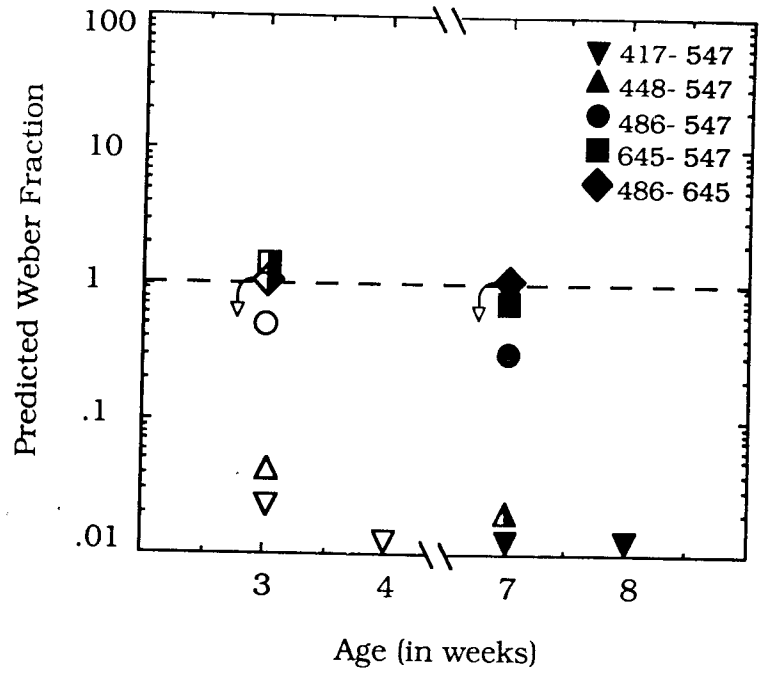

FIG. 1.17. Predictions of the visual efficiency hypothesis for the experiments of Clavadetscher et al. (1988) and Varner et al. (1985). Predicted Weber fractions are plotted for each of the test pairs used in those experiments. Conventions are the same as in Fig. 1.11 except that different symbols represent the different hue pairings. The solid arrows indicate that the predicted Weber fractions for those two points should be somewhat lower; see text for explanation.

(stimulus contrast required to elicit reliable discrimination) for each of the presented hue pairings. The horizontal line represents the stimulus contrast Clavadetscher et al. actually presented. Points above the horizontal line represent those conditions in which discrimination failures are predicted and those below the line the conditions in which discrimination successes are predicted. The filled symbols represent conditions in which discriminations were made reliably and unfilled symbols those conditions in which discriminations were consistently not made. Half-filled symbols represent those conditions in which there was some evidence for discrimination. The arrows next to the symbols for the 486/645 pairing (and the "less than" sign in Table 1.3) indicate that the predicted Weber fraction should be lower than the indicated values; Clavadetscher et al. presented the 486/645 pair at a higher luminance than the others. Decrement sensitivity probably improves with increasing luminance, changing the term LT_n in equations 1 and 2 presented earlier, which, in turn, would decrease the predict-

ed Weber fraction. Clavadetscher et al., however, did not measure intensity discrimination at the higher luminance, so we do not know how much the predictions should be displaced downward.

One can see from Fig. 1.17 that the hypothesis accurately predicts 7-week-olds' ability to distinguish four of the five hue pairings presented in the study. The hypothesis does not predict the 3-week data, however. It predicts correctly that 3-week-olds' ability to discriminate 645/547 and 486/red pairings should approach reliability, but it predicts incorrectly that these infants should discriminate the other pairings—417/547, 448/547, and 486/547—reliably. It is significant that these three pairings are the ones that most involve SWS cones. Consequently, as with Varner et al. (1985), we are forced to reject the visual efficiency hypothesis as an explanation for hue discriminations that involve the SWS cones. Instead, it looks like neonates have either relatively insensitive SWS cones or a relatively insensitive postreceptoral blue/yellow mechanism that subserves SWS cones.

The constellation of results suggests that the visual efficiency hypothesis accounts accurately for the development of hue discriminations that involve MWS and LWS cones, but fails to account for the development of discriminations that involve SWS cones. Thus, we hypothesize that human neonates have a tritan defect due to dysfunctional SWS cones or possibly to delayed development among the blue/yellow, postreceptoral chromatic mechanism. To pursue this idea, we created a neonatal ideal observer with no SWS cones in order to simulate a tritan defect. We then used exactly the same procedure, as outlined in equations 1 and 2, to generate predictions of discrimination performance in the conditions of Varner et al. (1985) and Clavadetscher et al. (1988). The visual efficiency hypothesis for an observer with a tritan defect predicts an inability to discriminate the 417/547 nm pairing in Varner et al. and Clavadetscher et al. because those lights stimulate MWS and LWS cones in the same ratio, so discrimination has to be based on differential activation of the SWS cones. The other predictions are portrayed in Fig. 1.18 (see also Table 1.4). As in previous figures with this format, the predicted Weber fraction (or stimulus contrast) needed to discriminate the lights is plotted for each hue pairing. The horizontal line represents the stimulus contrast actually presented in the Clavadetscher et al. study, so any points plotted above the line represent predicted discrimination failures and those below the line represent predicted discrimination successes. Filled symbols represent conditions in which infants made the hue discrimination reliably and open symbols the conditions in which they reliably did not make the discrimination. Half-filled symbols represent conditions in which there was modest evidence for discrimination.

Clearly, the tritan-defective predictions are accurate for the 3-week data, but, as expected, inaccurate for the 7-week data. They are therefore supportive of the idea that infants 4 weeks of age or younger have a tritan defect and

TABLE 1.4

Experiment	*Age*	*Task*	*Stimuli*	*Results*	*Ratio*	*Predicted Weber Fraction*	*Accurate Prediction*
Varner et al. (1985)	4 weeks	Intensity	Green(4°×4°)	Threshold = ± .16 lu			
		Chromatic	Violet on green	Fail	24.26	7.52	+
Clavadetscher et al. (1988)	3 weeks	Intensity	Green(8°×8°)	Threshold = ± .40 lu			
		Chromatic	Violet 1 on green	Fail	24.26	14.60	+
		Chromatic	Violet 2 on green	Fail	2.79	1.67	+
		Chromatic	Blue on green	Fail	3.44	2.07	+
		Chromatic	Red on green	Marginal	2.00	1.20	+
		Chromatic	Blue on red	Marginal	2.87	<1.72	+

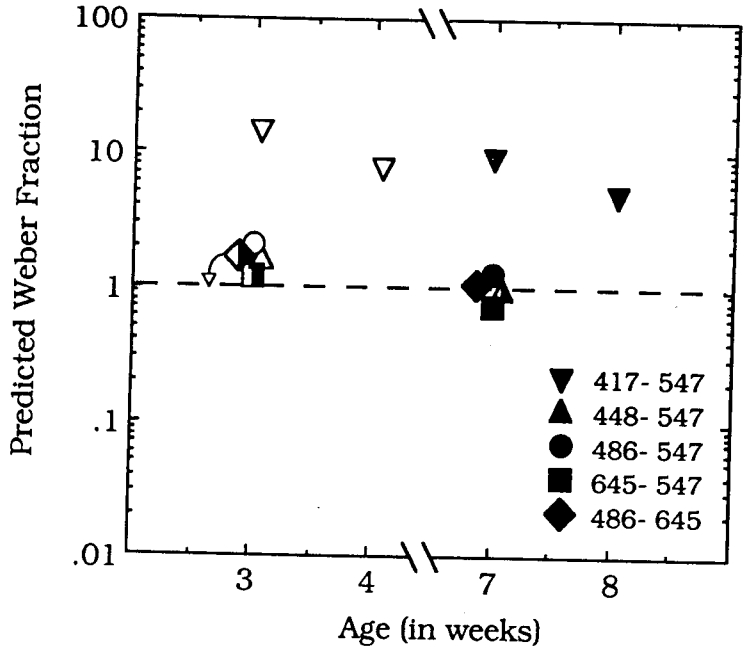

FIG. 1.18. Predictions for the visual efficiency hypothesis when SWS cones are assumed to be nonfunctional. Conventions are the same as in Fig. 1.17.

older infants do not. The early defect could be due to relative insensitivity among SWS cones or among postreceptoral blue/yellow chromatic mechanisms.

In summary, the predictions of the visual efficiency hypothesis are consistent with the pattern of Rayleigh and neutral-point discriminations observed by Teller et al. (1978). Moreover, Allen et al. (1990) have shown empirically that the chromatic information required to make a Rayleigh discrimination is transmitted to the cortex of infants as young as 2 weeks of age. Consequently, Rayleigh discrimination and most neutral-point failures observed among the youngest children and for small targets among the older children do not imply differential deficiencies among chromatic mechanisms per se. Rather, the ratio of chromatic to luminance sensitivity remains constant across age, as shown empirically by Allen et al. (1990) for Rayleigh discriminations, suggesting that neonates' apparent inability to make chromatic discriminations that depend solely on MWS and LWS cones is caused by an overall deficit in visual efficiency. The predictions of the visual efficiency hypothesis are not consistent with the tritan discriminations observed by Varner et al. (1985) and Clavadetscher et al. (1988). Modifying the visual efficiency hypothesis to include a tritan defect at 3 and 4 weeks allowed us to predict all of the data with reasonable accuracy. Therefore, young infants may, in fact, possess some form of color anomaly invoking a deficiency among SWS cones or cone pathways fed by them.

DISCUSSION

Ideal observer analyses were used to estimate the information available at the photoreceptors for the discrimination of spatial and chromatic stimuli. The information is much reduced in the human neonate compared to the adult mainly because of immaturities among neonates' photoreceptors. This reduction in the information available for discrimination sets an upper bound on the visual performance human neonates are capable of given their optics and photoreceptors. Real newborns can do no better than the neonatal ideal observer. The discrimination information lost by inefficient photoreception accounts for a substantial fraction of the gap between adult and infant contrast sensitivity, grating acuity, and chromatic discrimination. Nonetheless, the magnitude of the information gain with age is insufficient by itself to account for the entire developmental gap in these tasks.

In this section, we consider various hypotheses about the sources of the postreceptoral loss and the sorts of visual tasks for which this analysis is likely or unlikely to yield useful insights.

Contributors to Postreceptoral Loss

The performance of the neonatal ideal observer was much better than that of human neonates in all of the tasks considered. This is hardly surprising given that human adult performance does not equal ideal performance in these same tasks. More interestingly, the gap between real and ideal neonate values is significantly larger than that between real and ideal adult values (see Figs. 1.8 and 1.9). This means that neonates, although significantly limited by optical and receptoral deficiencies, use the information that is available at the photoreceptors less efficiently than adults do. What postreceptoral factors contribute to this additional developmental deficit? Some of the obvious candidates are considered here.

Before considering mechanistic explanations of postreceptoral loss, we should entertain a methodological explanation: Perhaps the sensitivity of the young visual system is actually better than believed, so the postreceptoral loss is properly ascribed to motivational deficiency. There is no good theory of how motivation should affect visual performance, so unfortunately, it is difficult to know where to look for its effects. For the sake of argument, though, suppose that behavioral estimates of visual thresholds are uniformly higher than true sensory thresholds. This would imply that the postreceptoral gap is smaller than our estimates. Behavioral procedures, like FPL, rely on an infant's willingness to perform the appropriate looking behavior. It is well known that infants tend to preferentially fixate patterned over unpatterned stimuli, but their looking preference is entirely voluntary and certainly not mandated whenever they detect a target. The VEP technique used in infant vision studies only requires that the infant look in the direction of the target for fairly brief periods. For these reasons, it has

been assumed that the FPL measurements are more subject to motivational deficits. VEP measurements commonly reveal greater sensitivities than behavioral measurements. For instance, grating acuity measured by VEP is typically an octave higher (Dobson & Teller, 1978). If this argument is accepted, it should be noted that VEP estimates of neonatal contrast sensitivity and grating acuity still fall well short of the values predicted from the front-end losses as plotted in Fig. 1.8.[3] That is to say, whether one relies on FPL or VEP measurements of visual sensitivity, one cannot explain all of the difference between neonatal and adult performance from front-end losses alone.

There are a number of possible explanations involving inefficient neural processing that might explain age changes in the postreceptoral loss. Real observers' deviations from ideal performance are characterized by two general factors: the level of internal noise and the efficiency with which the observer utilizes available stimulus information. These two factors have been called *intrinsic noise* and *sampling efficiency*, respectively (Legge, Kersten, & Burgess, 1987). Here the possibility is discussed that one or both of these causes of less-than-ideal performance contribute to the postreceptoral loss observed in neonates.

Intrinsic noise refers to sources of random error within the visual system. In an audio system, an example is a noisy amplifier. There are numerous sources of noise within the visual system that could degrade visual performance. Let us discuss one plausible example because it might be particularly important in developing systems. A consistent and striking physiological observation is that cells in the visual cortex of kittens respond sluggishly compared to adult cells (Bonds, 1979; Derrington & Fuchs, 1981; Hubel & Wiesel, 1963). Their response latency, fatigability, and peak firing rate are much lower than those found in mature neurons. The firing rates of retinal ganglion cells, in contrast, do not differ markedly across age (Hamasaki & Flynn, 1977). Peak firing rates also decrease at successive sites in the geniculostriate pathway of adult cats, but the effect is more dramatic in kittens. Thus, it appears that peak firing rate drops dramatically in the ascending visual pathway of kittens. The human visual cortex appears to be quite immature early in life, too (Atkinson & Braddick, 1981; Braddick & Atkinson, 1987; Naegele & Held, 1982), so the same drop in firing rate may occur in human neonates. Reduced firing rates from retina to cortex, if caused by random or nearly random dropping of spikes from one cell to the next, would decrease the total number of spikes in an unpredictable

[3]This discussion makes an important and incorrect assumption that the thresholds obtained with VEP are comparable to those obtained with FPL. The means of estimating VEP thresholds involves signal averaging and extrapolation of data, which are not used in FPL. We do not know how much averaging and extrapolation decreases the estimated threshold (i.e., increases estimated sensitivity), so one is really comparing apples and oranges in such a discussion. Our only point is that even with those enhancements, VEP estimates still fall short of ideal observer performance (which does not involve this sort of averaging and extrapolation).

way. If the spike trains are Poisson distributed (an approximation to the binomial distribution) or nearly so, a drop in the mean number of spikes reduces the signal-to-noise ratio. It is equivalent to adding noise and, therefore, is best thought of as a source of intrinsic noise. Thus, successive reductions in firing rate may well be a significant source of information loss in the young visual system.

Poor sampling efficiency may also contribute significantly to the postreceptoral loss. The optimal strategy in detecting a visual stimulus is one that extracts the greatest signal information possible while keeping the effects of external or internal noise to a minimum. When the parameters of the signal are known, the optimal strategy is implemented, for all intents and purposes, by a weighting function that matches the profile of the expected signal (for a rigorous treatment, see Geisler, 1989). This is probably accomplished in the visual system by monitoring the activity of neurons whose receptive fields nearly match the profile of the expected signal. The newborn visual system might exhibit poorer sampling efficiency than the adult for two reasons. First, because of the immaturity of the visual cortex, neurons with receptive fields that match experimental stimuli (e.g., sinewave gratings) may be rare or non-existent. Second, and perhaps most importantly, in behavioral experiments the situation is surely quite different for a neonate compared to an adult. The adult can be coached to anticipate the spatial configuration and temporal characteristics of the signal to be detected. Thus, an adult observer can choose more wisely which neurons to monitor. Newborns, on the other hand, cannot be coached in such a fashion. The experimenter has to rely on the general orienting response of the child to salient or novel targets. The child presumably has to monitor the activity of a very large number of neurons, any of which could indicate the appearance of a salient or novel event. The consequence is a reduction in sampling efficiency.

The contributions of intrinsic noise and sampling inefficiency to the postreceptoral gap can be distinguished by the so-called *equivalent noise paradigm* (Legge et al., 1987; Pelli, 1990). In this paradigm, observers are asked to detect targets embedded in a noise masker. The logic of the paradigm is portrayed in the left panel of Fig. 1.19. Hypothetical contrast thresholds for detecting a sinusoidal grating are plotted as a function of noise intensity. An ideal observer has no intrinsic noise and is able to sample the stimuli to be discriminated optimally; its contrast thresholds are proportional to noise spectral density. Real observers possess some amount of intrinsic noise and sample stimuli with less than perfect efficiency. One can see the effects of these two sources of information loss in the real observer curve in the left panel of the figure. At low noise intensities, the threshold-elevating effects of intrinsic noise are larger than those of the noise masker, so real observer thresholds at low noise levels are flat and elevated relative to ideal observer thresholds. As the intensity of the noise masker is increased, however, the elevating effects of the masker begin to override those of intrinsic noise. The noise level at which this occurs is called the *equivalent noise* because it is the level at which the masker's effects are

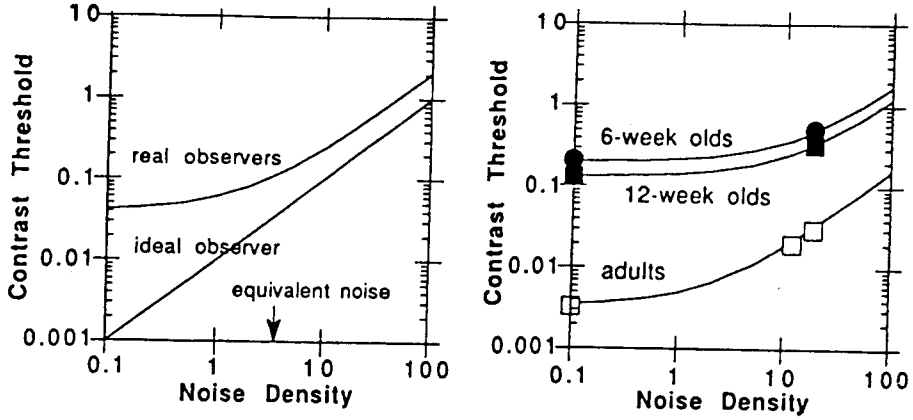

FIG. 1.19. Predicted and observed data in equivalent noise paradigm plots. Both panels plot contrast threshold for detecting a sinewave grating as a function of the strength of a noise masker. The left panel shows the expected functions for an ideal observer with no intrinsic noise and perfect sampling efficiency and that for a real observer with some intrinsic noise and imperfect sampling efficiency. The estimate of the equivalent noise strength is indicated by the arrow. The right panel shows the observed functions from an experiment by Banks, Stephens, and Hartmann (1985) for 6-week-olds, 12-week-olds, and adults.

equivalent to the effects of intrinsic noise. Finally, at high noise intensities, threshold becomes proportional to masker level. The gap between real and ideal performance here is a measure of sampling efficiency uncontaminated by intrinsic noise.

Banks, Stephens, and Hartmann (1985) provided some data relevant to measuring intrinsic noise and sampling inefficiency in young infants. This experiment, however, was conducted for another purpose, so there are too few measurements to draw any firm conclusions. Nonetheless, it is interesting to consider their findings. Banks et al. presented sinewave gratings with and without a noise masker to 6-week-olds, 12-week-olds, and adults. We have replotted their data in the right panel of Fig. 1.19. The data points on the left side of the figure are the contrast thresholds when the noise was not present and those on the right are the thresholds when different noise maskers were present. The key finding is that adults exhibited a significantly larger masking effect than did 6- or 12-week-olds. That is to say, the presence of the noise elevated threshold much more in adults than in infants. As shown in the plot in the right panel, this implies that the 6- and 12-week-olds have more intrinsic noise than adults do; stated another way, the equivalent noise in infants appears to be higher than in adults. It also appears from these plots that infant and adult curves will not superimpose at high noise levels, which if true, implies that infants' sampling efficiency is poorer, too.

As stated earlier, the spatial and chromatic visual deficits infants exhibit are due to both front-end and postreceptoral immaturities. The postreceptoral immaturities—whose effects are evidenced by the postreceptoral gap shown in Fig. 1.9—may well be caused by both elevated intrinsic noise and low sampling efficiency.

Developmental Findings That Do and Do Not Lend Themselves to Ideal Observer Analyses

According to Occam's razor, scientific explanations should be sought first in terms of known qualities. We have followed this philosophy by examining the information available at the photoreceptors for making a variety of spatial and chromatic discriminations and by calculating how the information at the photoreceptors changes with age. Thus, more complicated explanations involving different growth rates among retinal and cortical mechanisms (e.g., Shimojo & Held, 1987) are not required. We also found that neonates' inability to make a variety of chromatic discriminations is consistent with analyses of the information at the receptors. Consequently, explanations involving delayed development of chromatic mechanisms are not necessary (at least for LWS and MWS cones and for the red/green chromatic mechanism).

Only a subset of the spatial and chromatic tasks in the infant literature has been examined here. Indeed, the tasks chosen are ones in which real observers are most likely to behave similarly to ideal observers. This analysis would be inconsistent with observed behavior in a large number of other spatial and chromatic tasks. For example, spatial frequency and orientation masking (Blakemore & Campbell, 1969; Campbell & Kulikowski, 1966) occur at postreceptoral sites, so their development (Banks et al., 1985; Braddick, Wattam-Bell, & Atkinson, 1986) would not be evident in ideal observers like ours. Increment threshold functions (Barlow, 1958) follow Weber's law across a wide range of stimulus conditions. This lawful behavior is in part a manifestation of the operation of adaptation mechanisms, a factor not considered in this analysis. Consequently, an important aspect of the development of increment threshold functions (Dannemiller & Banks, 1983; Hansen & Fulton, 1981) will not be reflected in age changes in front-end limitations. Finally, the sensitivity roll-off and Weber's behavior of the low-frequency end of the mature CSF (Kelly, 1977) is commonly attributed to the operation of lateral interactions among retinal network mechanisms, another factor not considered here. Thus, the development of this property of the CSF (Atkinson et al., 1977; Banks & Salapatek, 1981; but see Movshon & Kiorpes, 1988) will also not be manifest in ideal observer performance.

The development of numerous spatial and chromatic capabilities, therefore, will not be evident in analyses of age changes in the information at the photo-

receptors. Nonetheless, ideal observer analyses might still be quite helpful in investigation of such capabilities. As pointed out by Watson (1987), even departures of real observers' performance from ideal are important clues about the structure of processing. Such departures show that human visual performance is influenced substantially by postreceptoral processes. Similarly, developmental changes in the departures between real and ideal performance indicate how post-receptoral contributions vary with age.

SUMMARY

We examined the contributions of pre-neural factors to the differences between neonatal and adult spatial and chromatic vision. Ideal observers were constructed that incorporated reasonable estimates of the optics, ocular media, and photoreceptor aperture, efficiency, and spacing of adult and neonatal foveas. Comparison of the performance of these ideal observers allowed us to estimate reasonably rigorously the contribution of optical and receptoral immaturities to the deficits in neonates' spatial and chromatic vision. There were two main findings:

1. Immaturities in pre-neural mechanisms alone (primarily reduced eye size and changes in photoreceptor morphology) predict a 1.3 log unit decrease in contrast sensitivity and 2-octave (.6 log unit) decrease in grating acuity. Although these are substantial effects, they are smaller than the observed differences: Grating acuity for 4-week-old infants, for example, is typically 3.5 to 4.5 octaves lower than the mature values. Therefore, we conclude that pre-neural mechanisms account for much, but not all, of the differences between neonatal and adult contrast sensitivity and grating acuity. The remaining difference must reflect the contribution of postreceptoral mechanisms.
2. The failure of infants younger than 7 weeks to make a variety of chromatic discriminations may be caused by poor visual efficiency rather than differential immaturities among cone types or chromatic channels. In addition, improvements in chromatic discrimination observed from birth to 12 weeks may reflect improvements in visual efficiency rather than in chromatic mechanisms. The hypothesis fails, however, to predict the inability of infants younger than 7 weeks to make chromatic discriminations that depend on SWS cones. We showed that those discrimination failures and subsequent improvements can be explained by assuming that SWS cones, or the postreceptoral circuits that serve them, are quite immature during the first weeks of life.

ACKNOWLEDGMENTS

This research was supported by NICHHD Research Grant HD-19927 to Martin S. Banks. We thank David Shen for his assistance in the preparation of the manuscript and Andrew Eisman for programming assistance. We are also grateful to Davida Teller and Carl Granrud for helpful comments on the manuscript.

REFERENCES

Abramov, I., Gordon, J., Hendrickson, A., Hainline, L., Dobson, V., & LaBossiere, E. (1982). The retina of the newborn human infant. *Science, 217,* 265–267.

Allen, D., Banks, M. S., Norcia, A. M., & Shannon, E. (1990). Human infants' VEP responses to isoluminant stimuli. *Investigative Ophthalmology and Visual Science, 31* (Suppl. 4), 10.

Allen, D., Norcia, A. M., & Tyler, C. W. (1989). Development of grating acuity and contrast sensitivity in the central and peripheral visual field of the human infant. *Investigative Ophthalmology and Visual Science, 30* (Suppl. 4), 311.

Atkinson, J., & Braddick, O. (1981). Development of optokinetic nystagmus in infants: An indicator of cortical binocularity? In D. F. Fisher, R. A. Monty, & J. W. Sanders (Eds.), *Eye movements: Cognition and visual perception* (pp. 53–64). Hillsdale, NJ: Lawrence Erlbaum Associates.

Atkinson, J., Braddick, O., & Moar, K. (1977). Development of contrast sensitivity over the first three months of life in the human infant. *Vision Research, 17,* 1037–1044.

Banks, M. S., & Bennett, P. J. (1988). Optical and photoreceptor immaturities limit the spatial and chromatic vision of human neonates. *Journal of the Optical Society of America A, 5,* 2059–2079.

Banks, M. S., & Dannemiller, J. L. (1987). Infant visual psychophysics. In P. Salapatek & L. B. Cohen (Eds.), *Handbook of infant perception: From sensation to perception* (pp. 115–184). New York: Academic Press.

Banks, M. S., Geisler, W. S., & Bennett, P. J. (1987). The physical limits of grating visibility. *Vision Research, 27,* 1915–1924.

Banks, M. S., & Salapatek, P. (1978). Acuity and contrast sensitivity in 1-, 2-, and 3-month-old human infants. *Investigative Ophthalmology and Visual Science, 17,* 361–365.

Banks, M. S., & Salapatek, P. (1981). Infant pattern vision: A new approach based on the contrast sensitivity function. *Journal of Experimental Child Psychology, 31,* 1–45.

Banks, M. S., & Salapatek, P. (1983). Infant visual perception. In M. M. Haith & J. J. Campos (Eds.), *Handbook of child psychology* (pp. 435–571). New York: Wiley.

Banks, M. S., Stephens, B. R., & Hartmann, E. E. (1985). The development of basic mechanisms of pattern vision: Spatial frequency channels. *Journal of Experimental Child Psychology, 40,* 501–527.

Barlow, H. B. (1958). Temporal and spatial summation in human vision at different background intensities. *Journal of Physiology, 141,* 337–350.

Blakemore, C., & Campbell, F. W. (1969). On the existence of neurons in the human visual system selectively sensitive to the orientation and size of retinal images. *Journal of Physiology, 203,* 237–260.

Blakemore, C., & Vital-Durand, F. (1980). Development of the neural basis of visual acuity in monkeys: Speculation on the origin of deprivation amblyopia. *Transactions of the Ophthalmological Society of the United Kingdom, 99,* 363–368.

Bonds, A. B. (1979). Development of orientation tuning in the visual cortex of kittens. In R. Freeman (Ed.), *Developmental neurobiology of vision* (pp. 31–41). New York: Plenum.

Bone, R. A., Landrum, J. T., Fernandez, L., & Tsarsis, S. L. (1988). Analysis of the macular pigment by HPLC: Retinal distribution and age study. *Investigative Ophthalmology and Visual Science, 29,* 843–849.

Booth, R. G., Williams, R. A., Kiorpes, L., & Teller, D. Y. (1980). Development of contrast sensitivity in infant *Maccaca nemestrina* monkeys. *Science, 208,* 1290–1292.

Braddick, O., & Atkinson, J. (1987). Sensory selectivity, attentional control, and cross-channel integration in early visual development. In A. Yonas (Ed.), *Perceptual development in infancy: The Minnesota Symposium on Child Psychology* (pp. 105–143). Hillsdale, NJ: Lawrence Erlbaum Associates.

Braddick, O., Wattam-Bell, J., & Atkinson, J. (1986). Orientation specific cortical responses develop early in infancy. *Nature, 320,* 617–619.

Bronson, G. W. (1974). The postnatal growth of visual capacity. *Child Development, 45,* 874–890.

Brown, A. M., Dobson, V., & Maier, J. (1987). Visual acuity of human infants at scotopic, mesopic and photopic luminances. *Vision Research, 27,* 1845–1858.

Campbell, F. W., & Gubisch, R. W. (1966). Optical quality of the human eye. *Journal of Physiology, 186,* 558–578.

Campbell, F. W., & Kulikowski, J. J. (1966). Orientation selectivity of the human visual system. *Journal of Physiology, 187,* 437–445.

Clavadetscher, J. M., Brown, A. M., Ankrum, C., & Teller, D. Y. (1988). Spectral sensitivity and chromatic discrimination in 3- and 7-week-old human infants. *Journal of the Optical Society of America A, 5,* 2093–2105.

Coletta, N. J., Williams, D. R., & Tiana, C. L. M. (1990). Consequences of spatial sampling for human motion perception. *Vision Research, 30,* 1631–1648.

Cornsweet, T. (1970). *Visual perception.* Orlando, FL: Harcourt Brace Jovanovich.

Crowell, J. A., & Banks, M. S. (1991). *The efficiency of foveal vision.* Manuscript submitted for publication.

Dannemiller, J. L., & Banks, M. S. (1983). The development of light adaptation in human infants. *Vision Research, 23,* 599–610.

Derrington, A. M., & Fuchs, A. F. (1981). The development of spatial-frequency selectivity in kitten striate cortex. *Journal of Physiology, 316,* 1–10.

Dobson, V., & Teller, D. Y. (1978). Visual acuity in human infants: A review and comparison of behavioral and electrophysiological techniques. *Vision Research, 18,* 1469–1483.

Estevez, O. (1979). *On the fundamental data-base of normal and dichromatic color vision.* Unpublished doctoral dissertation, University of Amsterdam, The Netherlands.

Geisler, W. S. (1984). Physical limits of acuity and hyperacuity. *Journal of the Optical Society of America A, 1,* 775–782.

Geisler, W. S. (1989). Sequential ideal-observer analysis of visual discriminations. *Psychological Review, 96,* 267–314.

Green, D. G. (1970). Regional variations in the visual acuity for interference fringes on the retina. *Journal of Physiology, 207,* 351–356.

Green, D. M., & Swets, J. A. (1966). *Signal detection theory and psychophysics.* New York: Robert E. Krieger.

Hainline, L., Harris, C. M., & Krinsky, S. J. (1990). Variability of refixations in infants. *Infant Behavior and Development, 13,* 321–342.

Hamaski, D. I., & Flynn, J. T. (1977). Physiological properties of retinal ganglion cells of 3-week-old kittens. *Vision Research, 17,* 275–284.

Hamer, R. D., Alexander, K., & Teller, D. Y. (1982). Rayleigh discriminations in young human infants. *Vision Research, 22,* 575–588.

Hansen, R. M., & Fulton, A. B. (1981). Behavioral measurement of background adaptation in infants. *Investigative Ophthalmology and Visual Science, 21,* 621–629.

Hendrickson, A., & Kupfer, C. (1976). The histogenesis of the fovea in the macaque monkey. *Investigative Ophthalmology, 15,* 746–756.

Hickey, T. L., & Peduzzi, J. D. (1987). Structure and development of the visual system. In P. Salapatek & L. B. Cohen (Eds.), *Handbook of infant perception: From sensation to perception* (pp. 1–42). New York: Academic Press.

Hirano, S., Yamamoto, Y., Takayama, H., Sugata, Y., & Matsuo, K. (1979). Ultrasonic observations of eyes in premature babies: Part 6. Growth curves of ocular axial length and its components. *Acta Societatis Ophthalmologicae Japonicae, 83,* 1679–1693.

Howell, E. R., & Hess, R. F. (1978). The functional area for summation to threshold for sinusoidal gratings. *Vision Research, 18,* 369–374.

Hubel, D. H., & Wiesel, T. N. (1963). Receptive fields of cells in striate cortex of very young, visually inexperienced kittens. *Journal of Neurophysiology, 26,* 994–1002.

Jacobs, D. S., & Blakemore, C. (1988). Factors limiting the postnatal development of visual acuity in the monkey. *Vision Research, 28,* 947–958.

Kelly, D. H. (1977). Visual contrast sensitivity. *Optica Acta, 24,* 107–129.

Kiely, P. M., Crewther, S. G., Nathan, J., Brennan, N. A., Efron, N., & Madigan, M. (1987). A comparison of ocular development of the cynomolgus monkey and man. *Clinical Visual Science, 3,* 269–280.

Larsen, J. S. (1971). The sagittal growth of the eye: IV. Ultrasonic measurement of the axial length of the eye from birth to puberty. *Acta Ophthalmologica, 49,* 873–886.

Legge, G., Kersten, D., & Burgess, A. E. (1987). Contrast discrimination in noise. *Journal of the Optical Society of America A, 4,* 391–404.

Lewis, T. L., Maurer, D., & Kay, D. (1978). Newborns' central vision: Whole or hole? *Journal of Experimental Child Psychology, 26,* 193–203.

Movshon, J. A., & Kiorpes, L. (1988). Analysis of the development of contrast sensitivity in monkey and human infants. *Journal of the Optical Society of America A, 5,* 2166–2172.

Mullen, K. T. (1985). The contrast sensitivity of human color vision to red/green and blue/yellow chromatic gratings. *Journal of Physiology, 359,* 381–400.

Naegele, J. R., & Held, R. (1982). The postnatal development of monocular optokinetic nystagmus in infants. *Vision Research, 22,* 341–346.

Norcia, A. M., & Tyler, C. W. (1985). Spatial frequency sweep VEP: Visual acuity during the first year of life. *Vision Research, 25,* 1399–1408.

Norcia, A. M., Tyler, C. W., & Allen, D. (1986). Electrophysiological assessment of contrast sensitivity in human infants. *American Journal of Optometry and Physiological Optics, 63,* 12–15.

Packer, O., Hartmann, E. E., & Teller, D. Y. (1984). Infant color vision: The effect of test field size on Rayleigh discriminations. *Vision Research, 24,* 1247–1260.

Peeples, D. R., & Teller, D. Y. (1975). Color vision and brightness discrimination in two-month-old infants. *Science, 189,* 1102–1103.

Pelli, D. (1990). Quantum efficiency of visicn. In C. Blakemore (Ed.), *Vision: Coding and efficiency* (pp. 3–24). New York: Cambridge University Press.

Pirchio, M., Spinelli, D., Fiorentini, A., & Maffei, L. (1978). Infant contrast sensitivity evaluated by evoked potentials. *Brain Research, 141,* 179–184.

Rose, A. (1942). The relative sensitivities of television pick-up tubes, photographic film, and the human eye. *Proceedings of Institute of Radio Engineers, 30,* 293–300.

Salapatek, P. (1975). Pattern perception in early infancy. In P. Salapatek & L. B. Cohen (Eds.), *Infant perception: From sensation to cognition* (pp. 133–234). New York: Academic Press.

Salapatek, P., & Kessen, W. (1966). Visual scanning of triangles by the human newborn. *Journal of Experimental Child Psychology, 3,* 155–167.

Shimojo, S., & Held, R. (1987). Vernier acuity is less than grating acuity in 2- and 3-month-olds. *Vision Research, 27,* 77–86.

Slater, A. M., & Findlay, J. M. (1975). Binocular fixation in the newborn baby. *Journal of Experimental Child Psychology, 20,* 248–273.

Teller, D. Y., & Bornstein, M. H. (1987). Infant color vision and color perception. In L. B. Cohen & P. Salapatek (Eds.), *Handbook of infant perception: From sensation to perception* (pp. 185–236). New York: Academic Press.

Teller, D. Y., Peeples, D. R., & Sekel, M. (1978). Discrimination of chromatic from white light by two-month-old infants. *Vision Research, 18,* 41–48.

Varner, D., Cook, J. E., Schneck, M. R., McDonald, M. A., & Teller, D. Y. (1985). Tritan discriminations by 1- and 2-month-old human infants. *Vision Research, 25,* 821–832.

Walraven, P. L. (1974). A closer look at the tritanopic convergence point. *Vision Research, 14,* 1339–1343.

Watson, A. B. (1987). The ideal observer concept as a modeling tool. In *Frontiers of visual science: Proceedings of the 1985 Symposium* (pp. 32–37). Washington, DC: National Academy of Sciences.

Watson, A. B., Barlow, H. B., & Robson, J. G. (1983). What does the eye see best? *Nature, 31,* 419–422.

Werner, J. S. (1982). Development of scotopic sensitivity and the absorption spectrum of the human ocular media. *Journal of the Optical Society of America, 72,* 247–258.

Williams, D. R. (1985). Aliasing in human foveal vision. *Vision Research, 25,* 195–206.

Wilson, H. R. (1988). Development of spatiotemporal mechanisms in infant vision. *Vision Research, 28,* 611–628.

Yuodelis, C., & Hendrickson, A. (1986). A qualitative and quantitative analysis of the human fovea during development. *Vision Research, 26,* 847–876.